Lanni JS and Jacks T. (1998). *Mol. Cell Biol.*, **18,** 1055–1064.
Margolis RL, Lohez OD and Andreassen PR. (2003). *J. Cell Biochem.*, **88,** 673–683.
Marumoto T, Honda S, Hara T, Nitta M, Hirota T, Kohmura E and Saya H. (2003). *J. Biol. Chem.*, **278,** 51786–51795.
Meraldi P, Honda R and Nigg EA. (2002). *EMBO J.*, **21,** 483–492.
Minn AJ, Boise LH and Thompson CB. (1996). *Genes Dev.*, **10,** 2621–2631.
Nicklas RB. (1997). *Science*, **275,** 632–637.
Nishiyama Y, Hirota T, Morisaki T, Hara T, Marumoto T, Iida S, Makino K, Yamamoto H, Hiraoka T, Kitamura N and Saya H. (1999). *FEBS Lett.*, **459,** 159–165.
Shackney SE, Smith CA, Miller BW, Burholt DR, Murtha K, Giles HR, Ketterer DM and Pollice AA. (1989). *Cancer Res.*, **49,** 3344–3354.
Shah JV and Cleveland DW. (2000). *Cell*, **103,** 997–1000.
St John MA, Tao W, Fei X, Fukumoto R, Carcangiu ML, Brownstein DG, Parlow AF, McGrath J and Xu T. (1999). *Nat. Genet.*, **21,** 182–186.
Tao W, Zhang S, Turenchalk GS, Stewart RA, St John MA, Chen W and Xu T. (1999). *Nat. Genet.*, **21,** 177–181.
Toyn JH and Johnston LH. (1994). *EMBO J.*, **13,** 1103–1113.
Tugendreich S, Tomkiel J, Earnshaw W and Hieter P. (1995). *Cell*, **81,** 261–268.
Xia H, Qi H, Li Y, Pei J, Barton J, Blackstad M, Xu T and Tao W. (2002). *Oncogene*, **21,** 1233–1241.
Yang X, Li DM, Chen W and Xu T. (2001). *Oncogene*, **20,** 6516–6523.
Yasui Y, Amano M, Nagata K, Inagaki N, Nakamura H, Saya H, Kaibuchi K and Inagaki M. (1998). *J. Cell Biol.*, **143,** 1249–1258.

Acceleration of the Healing Process and Myocardial Regeneration May Be Important as a Mechanism of Improvement of Cardiac Function and Remodeling by Postinfarction Granulocyte Colony–Stimulating Factor Treatment

Shinya Minatoguchi, MD; Genzou Takemura, MD; Xue-Hai Chen, MD; Ningyuan Wang, MD; Yoshihiro Uno, MD; Masahiko Koda, MD; Masazumi Arai, MD; Yu Misao, MD; Chuanjiang Lu, MD; Koji Suzuki, MD; Kazuko Goto, BSc; Ai Komada, BSc; Tomoyuki Takahashi, PhD; Kenichiro Kosai, MD; Takako Fujiwara, MD; Hisayoshi Fujiwara, MD

Background—We investigated whether the improvement of cardiac function and remodeling after myocardial infarction (MI) by granulocyte colony–stimulating factor (G-CSF) relates to acceleration of the healing process, in addition to myocardial regeneration.

Methods and Results—In a 30-minute coronary occlusion and reperfusion rabbit model, saline (S) or 10 $\mu g \cdot kg^{-1} \cdot d^{-1}$ of human recombinant G-CSF (G) was injected subcutaneously from 1 to 5 days after MI. Smaller left ventricular (LV) dimension, increased LV ejection fraction, and thicker infarct-LV wall were seen in G at 3 months after MI. At 2, 7, and 14 days and 3 months after MI, necrotic tissue areas were 14.2±1.5/13.4±1.1, 0.4±0.1/1.8±0.5*, 0/0, and 0/0 $mm^2 \cdot slice^{-1} \cdot kg^{-1}$, granulation areas 0/0, 4.0±0.7/8.5±1.0*, 3.9±0.8/5.7±0.7,* and 0/0 $mm^2 \cdot slice^{-1} \cdot kg^{-1}$, and scar areas 0/0, 0/0, 0/0, and 4.2±0.5/7.9±0.9* $mm^2 \cdot slice^{-1} \cdot kg^{-1}$ in G and S, respectively (*$P<0.05$, G versus S). Clear increases of macrophages and of matrix metalloproteinases (MMP) 1 and 9 were seen in G at 7 days after MI. This suggests that G accelerates absorption of necrotic tissues via increase of macrophages and reduces granulation and scar tissues via expression of MMPs. Meanwhile, surviving myocardial tissue areas within the risk areas were significantly increased in G despite there being no difference in LV weight, LV wall area, or cardiomyocyte size between G and S. Confocal microscopy revealed significant increases of cardiomyocytes with positive 3,3,3′,3′-tetramethylindocarbocyanine perchlorate and positive troponin I in G, suggesting enhanced myocardial regeneration by G.

Conclusions—The acceleration of the healing process and myocardial regeneration may play an important role for the beneficial effect of post-MI G-CSF treatment. **(*Circulation*. 2004;109:2572-2580.)**

Key Words: myocytes ■ ischemia ■ reperfusion ■ matrix metalloproteinase

Granulocyte colony–stimulating factor (G-CSF), which can mobilize multipotential progenitor cells of bone marrow (BM) into peripheral blood, may improve post–myocardial infarction (MI) left ventricular (LV) remodeling and function. At present, the main mechanism is believed to be transdifferentiation of BM progenitor cells into the cell lineages of the heart, including cardiomyocytes, endothelial cells, etc, in the MI tissues.[1,2] However, recent studies have suggested that the transdifferentiation of c-Kit–positive BM cells into cardiomyocytes is controversial[3] and the number of the transdifferentiated cardiomyocytes from BM stem cells may be too low to explain the improvement of cardiac remodeling and function.[4]

The healing process after MI begins from absorption of necrotic tissues (acute stage: within several days after MI), moves into granulation with numerous myofibroblasts, rich microvessels, and collagen (subacute stage: 1 to 3 weeks after MI), and then forms scar tissues consisting primarily of collagen, with rare vessels via apoptosis of granulation cells (chronic stage: >1 month).[5] However, to the best of our knowledge, the precise quantitative studies on the dynamic changes of the above-described tissue factors are rare. Orlic et al[6] reported that scar tissue areas were reduced after G-CSF treatment, although the mechanism and the role were not examined. In the field of dermatology, it has been established that G-CSF enhances the

Received September 2, 2003; de novo received December 5, 2003; accepted February 20, 2004.

From the Second Department of Internal Medicine, Gifu University School of Medicine, Gifu (S.M., G.T., X.-H.C., N.W., Y.U., M.K., M.A., Y.M., C.L., K.S., H.F.); the Department of Cardiovascular Regeneration, Gifu University School of Medicine, Gifu (K.G., T.T., K.K.); and Kyoto Women's University, Kyoto (A.K., T.F.), Japan.

Correspondence to Hisayoshi Fujiwara, MD, Second Department of Internal Medicine, Gifu University School of Medicine, 40 Tsukasa Machi, Gifu 500-8705, Japan. E-mail gifuim-gif@umin.ac.jp

Circulation is available at http://www.circulationaha.org

DOI: 10.1161/01.CIR.0000129770.93985.3E

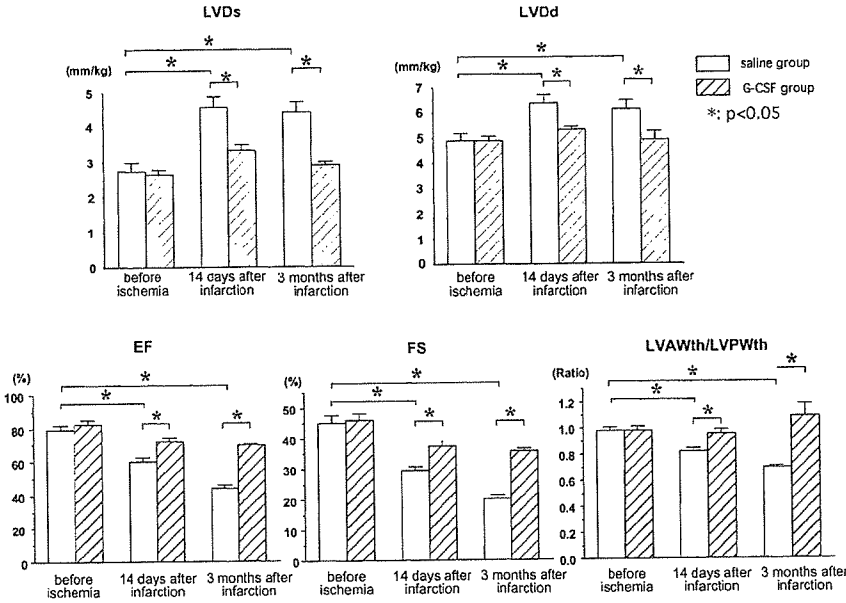

Figure 1. Echocardiographic data 14 days and 3 months after infarction. Note improvement of remodeling and function in G-CSF group. LVDs indicates LV systolic diameter; LVDd, LV diastolic diameter; EF, ejection fraction; FS, fractional shortening; LVAWth, LV anterior wall thickness; and LVPWth, LV posterior wall thickness.

healing process of various types of skin wounds via expression of various cytokines, such as the matrix metalloproteinase (MMP) family.[7-9] We hypothesized that G-CSF may also accelerate the healing process of MI wounds and that the acceleration may play an important role in the beneficial effects. Thus, the purpose of the present study was to define whether post-MI G-CSF treatment modifies the healing process via expression of MMPs, in addition to regeneration of myocardial tissues.

Methods

In this study, all rabbits received humane care in accordance with the *Guide for the Care and Use of Laboratory Animals*, published by the US National Institutes of Health (NIH publication 8523, revised 1985). The study protocol was approved by the Ethical Committee of Gifu University School of Medicine, Gifu, Japan.

The standard methods of 30-minute coronary arterial occlusion and reperfusion in male Japanese White rabbits weighing 1.9 to 2.2 kg were performed as previously reported.[10] Briefly, under anesthesia and mechanical ventilation with room air, a left thoracotomy was performed, and 4-0 silk string was placed beneath the large coronary arterial branch coursing down the middle of the anterolateral surface of the left ventricle. Then, the rabbits were killed by an overdose of pentobarbital after heparinization (500 U/kg).

Protocol 1

The subjects were 120 rabbits with 30-minute ischemia and 2-day, 7-day, 14-day, or 3-month reperfusion as described above. Saline at 0.5 mL in the saline group or 10 $\mu g \cdot kg^{-1} \cdot d^{-1}$ of recombinant human G-CSF (Lenograstin, Chugai Pharmaceutical Co, Ltd, Tokyo, Japan) in the G-CSF group starting 24 hours after infarction once per day for 5 days was administered subcutaneously in the 7-day groups (n=15 each in the saline and G-CSF groups), the 14-day groups (n=15 in each), and the 3-month groups (n=15 in each), but that in the 2-day groups (n=15 in each) was administered only once at 24 hours after infarction, when each rabbit was enrolled in the saline or G-CSF group by lot.

Echocardiography

Echocardiography (SSD2000, Aloka Co Ltd) and the measurement of arterial blood pressure were performed before and 14 days after MI in the 14-day groups (n=15 in each of the saline and G-CSF groups) and before and 3 months after MI in the 3-month groups (n=15 in each). The measurements were performed by 2 persons blinded to treatment.

Blood Sampling

Blood samples (0.3 mL each) were taken from an ear vein before and 7 days after MI in the 7-day groups (n=15 each in the saline and G-CSF groups) and before and 14 days after MI in the 14-day groups (n=15 in each) for peripheral blood cell counts and hemograms.

Pathology

The excised hearts of a total of 120 rabbits were mounted on a Langendorff apparatus, and Evans blue dye at 4°C was injected for 1 minute from the aorta after reocclusion of the coronary branch by a silk string for the measurement of risk areas. Then, the whole heart was perfused with 10% buffered formalin (4°C) for 2 minutes. The LV was weighed and sectioned into ≈7 transverse slices parallel to the atrioventricular ring. Each slice was fixed with 10% buffered formalin for 4 hours, embedded in paraffin, and sectioned with a microtome (4 μm thick). These sections were stained with hematoxylin-eosin and Sirius red. Under light microscopy, the risk area without blue dye, nonrisk area with blue dye, necrotic areas, granulation areas, and scar areas were clearly demarcated on the above-described stained preparations.

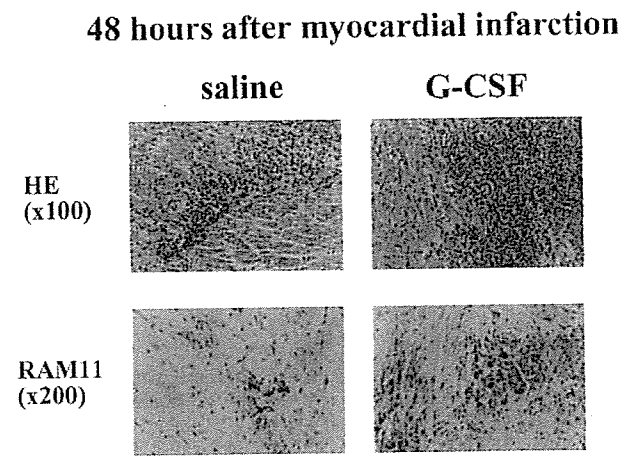

Figure 2. Histology of border zone between surviving area (left) and infarction (right). Note that acute inflammatory cell infiltration by hematoxylin-eosin (HE) stain and number of macrophages with positive RAM 11 stained with brown are clearly greater in G-CSF group.

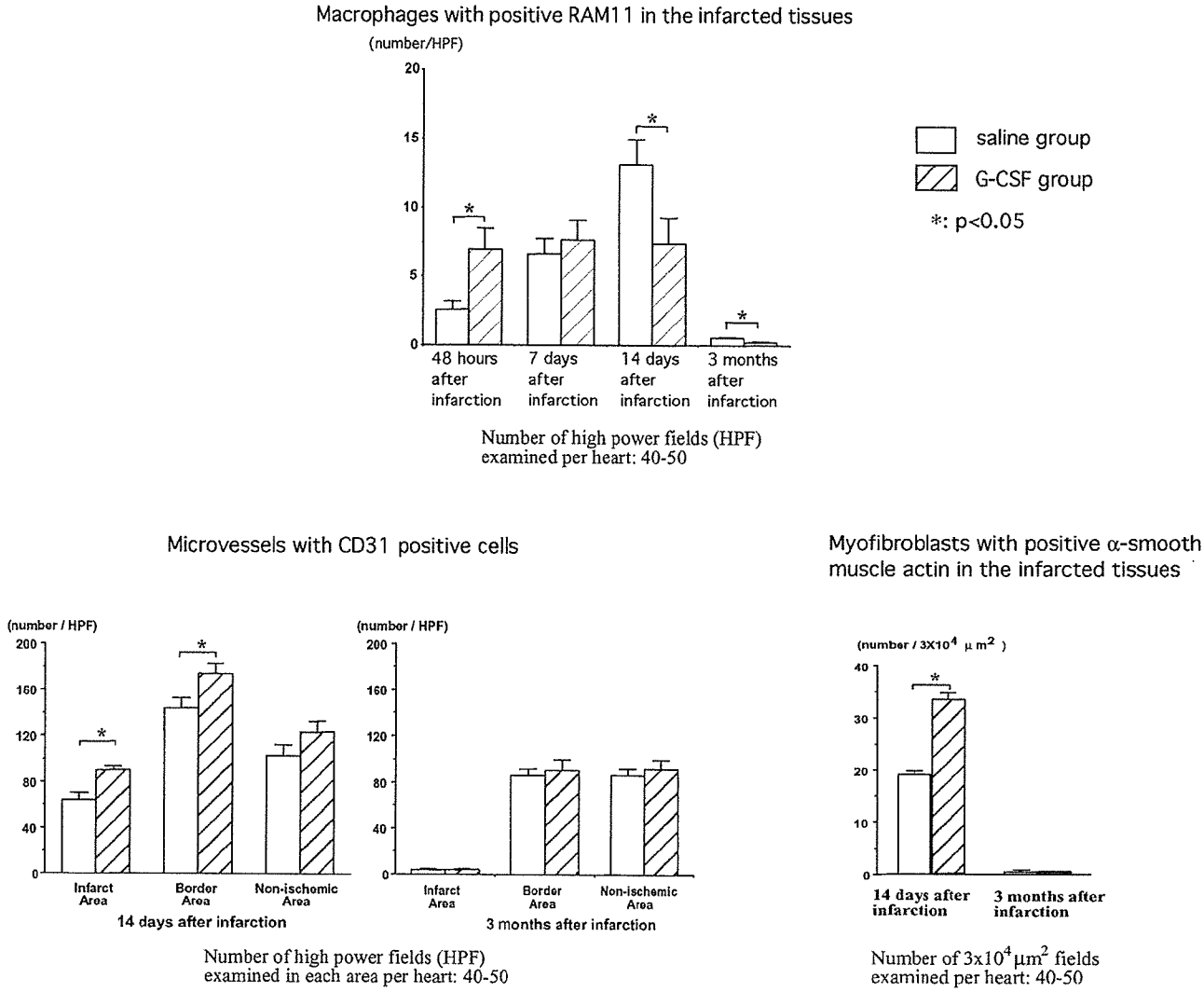

Figure 3. Quantitative analyses of macrophages, endothelial cells, and myofibroblasts

On the transversely sliced preparations with infarction in each heart, LV wall area, risk area, necrotic areas, granulation areas, scar areas, infarct areas, surviving areas in the risk areas, and collagen areas with positive Sirius red were calculated by use of an image analyzer connected to a light microscope (Luzex-F, Nireco) and were expressed as mm^2/slice/body weight (kg) corrected by mean risk area of each group for precise comparison. These were performed by 2 persons blinded to treatment.

Immunohistochemistry

By use of an indirect immunoperoxidase method, immunohistochemical stainings were performed using monoclonal mouse anti-troponin I antibody (Chemicon International, Inc) at 1:10, monoclonal mouse anti-human CD31, endothelial cell antibody (Dako) at 1:100, monoclonal mouse anti-human α-smooth muscle actin (Dako smooth muscle actin, 1A4) at 1:250, monoclonal mouse anti-macrophage antibody (Dako RAM11) at 1:100 and monoclonal mouse anti-human MMP1 antibody (Daiichi Fine Chemical Co Ltd, F-67) at 1:400, each of which cross-reacts with rabbit tissues. Morphometric analyses were performed by 2 persons blinded to treatment.

Protocol 2

In 14 rabbits, BM (≈10 mL) was aspirated from the right and left iliac crests 2 days before ischemia-reperfusion. To evaluate the incorporation of BM cells into the myocardium, BM mononuclear cells were labeled with fluorescent carbocyanine 1,1′-dioctadecyl-1-3,3,3′,3′-tetramethylindocarbocyanine perchlorate (DiI).[11] The DiI-labeled autologous BM mononuclear cells (≈1×10^7 cells) were returned into the BM space in the right and left iliac crests of each rabbit. Two days later, 30-minute ischemia and reperfusion was performed. Then, the saline group (n=7) and the G-CSF group (n=7) were made up by the same method as shown above and killed 14 days after MI. In addition, 7 other rabbits, as a negative control in which non–DiI-labeled BM cells were returned to BM of iliac crests, were killed 14 days after MI.

The hearts excised 14 days after MI were placed in iced PBS at <4°C immersion immediately after the animals were killed. The tissues (≈3×3×2 mm each) obtained from the risk area, including MI, and from the nonrisk area (3 tissues each) of each heart were embedded in OCT compound (Miles Scientific) and snap-frozen in liquid nitrogen. The OCT compound tissues were sectioned at 4-μm thickness with a cryostat for immunohistochemical analysis. In addition, the BMs of iliac crests were examined immunohistochemically.

Immunohistochemical staining was performed with Hoechst 33342 for nuclear staining, in addition to those detailed above. These were observed with confocal microscopy (LSM510 NLO, Zeiss), which can simultaneously analyze the relation among 3 different fluorescences and phase-contrast illustration. Morphometric analyses were performed by 2 persons blinded to treatment.

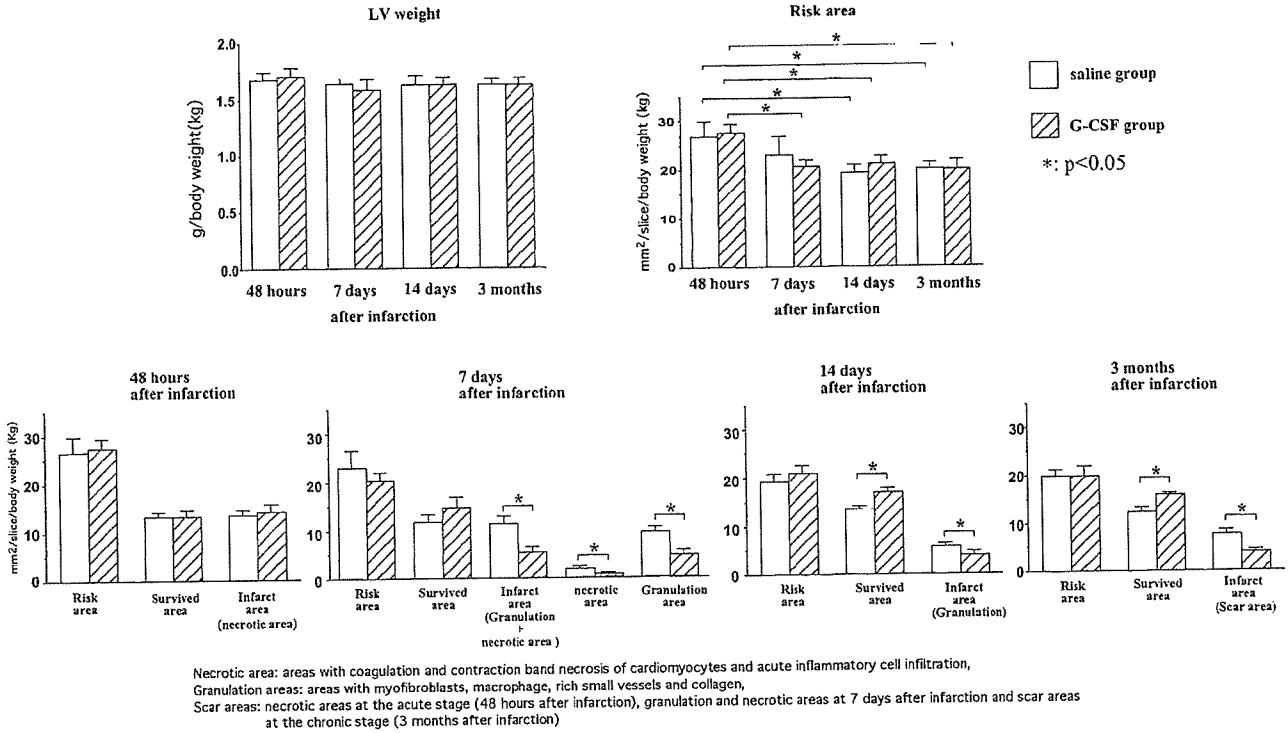

Figure 4. Time-course changes of LV weight, risk area, surviving area, infarct area, necrotic area, granulation area, and scar area after infarction

Protocol 3

Other saline (n=7) and G-CSF (n=7) groups with 30-minute ischemia and 7-day reperfusion and a sham group (n=7) were prepared for the measurement of MMP-1 and 9. The excised hearts were placed in iced PBS at <4°C immersion immediately after the animals were killed. Tissues of ≈200 mg each obtained from the center of the risk area and from the nonrisk area of LV wall were snap-frozen in liquid nitrogen.

For the measurement of MMP-1, a collagenase, ≈50 mg of the above-described frozen tissues obtained from each heart of the sham, saline, and G-CSF groups, was homogenized in lysis buffer and centrifuged at 10 000g at 4°C for 10 minutes. MMP-1 was measured by Western blot analysis using anti-human MMP-1 mouse monoclonal antibody (Daiichi Fine Chemical Co, F-67, clone No. 41-1E5). The signals were quantified by densitometry. The measurement of MMP-9, a gelatinase, in the remaining samples of the above-described frozen tissues was performed by zymography using the recommended methods of the Gelatinzymo electrophoresis kit (Yagai Research Center).

Statistical Analysis

All values are presented as mean±SEM. The differences between the saline and G-CSF groups were assessed by 2-way repeated-measures ANOVA. Differences at $P<0.05$ were considered statistically significant.

Results

Mortality

All rabbits in the 3-month saline and G-CSF groups enrolled 24 hours after MI survived during 3 months of experimentation.

Echocardiography and Blood Pressure

As shown in Figure 1, echocardiography showed a significant decrease in the LV end-systolic and LV end-diastolic dimensions and significant increases in the LV ejection fraction and fractional shortening in the G-CSF group compared with those of the saline group at 14 days and 3 months after MI. The ratio of the anterior LV wall thickness with infarction to the posterior wall thickness without infarction was greater in the G-CSF group than in the saline group. These suggest the improvements of LV remodeling and function by G-CSF. There was no significant difference in heart rate or blood pressure between the 2 groups (data not shown).

Peripheral Blood Cell Counts

White blood cells, granulocytes, and monocytes increased from 8800±588, 4021±278, and 357±91 before MI to 19 537±2641, 12 076±2663, and 1351±196/μL at 7 days after MI in the G-CSF group and were restored to 10 363±764, 5106±575, and 449±115/μL at 14 days after MI, respectively. There was no significant change in lymphocytes, red blood cells, or thrombocytes throughout the experiment. The saline group showed no significant changes.

General Histology

At 2 days after MI, large necrotic tissue areas were surrounded by numerous acute inflammatory cell infiltrations consisting of neutrophils, lymphocytes, and macrophages with positive RAM 11 in both the saline and G-CSF groups. However, the extent and density were clearly greater in the G-CSF group than in the saline group (Figure 2).

At 7 days after MI, necrotic tissue areas became smaller and acute infiltrated inflammatory cells were markedly reduced compared with the 2-day groups. The MI areas were to a large extent replaced by granulation in both the saline and G-CSF groups. At 14 days after MI, necrotic tissues were

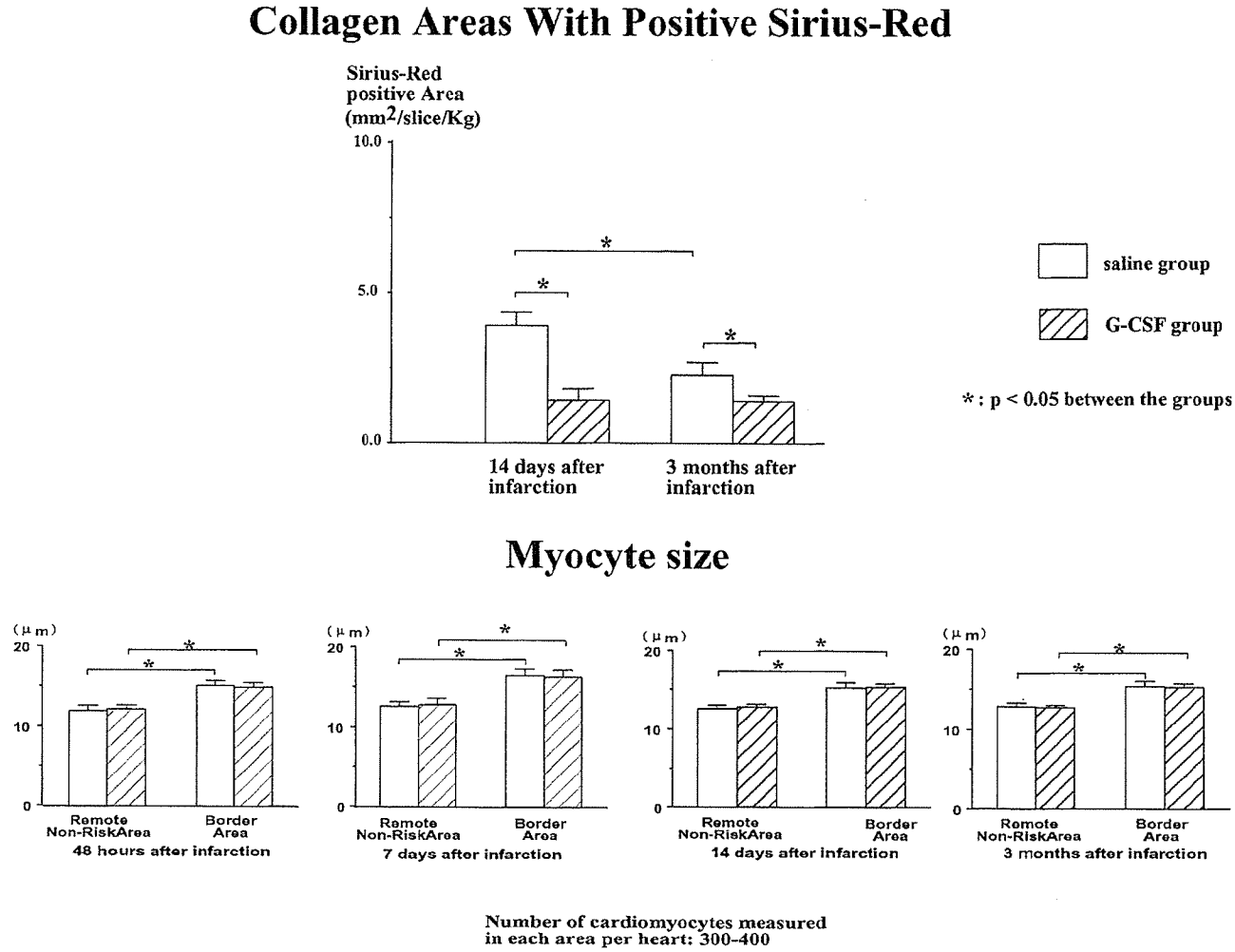

Figure 5. Collagen area with positive Sirius red and transverse size of cardiomyocytes

completely absorbed, and granulation tissues alone were observed in the saline and G-CSF groups. The densities of the myofibroblasts with positive α-smooth muscle actin and vessels with positive CD31 were clearly increased in the G-CSF group compared with those of the saline groups (Figure 3). The number of macrophages with positive RAM 11 was increased in the saline groups according to the duration of 2, 7, and 14 days (Figure 3). Meanwhile, it was similar in the G-CSF groups among the 3 durations. Thus, the number of macrophages was significantly greater in the G-CSF group than the saline group at 2 days after MI, similar at 7 days after MI, and lower in the G-CSF group than in the saline group at 14 days after MI (Figure 3).

At 3 months after MI, the granulation tissues were replaced by scar in each of the saline and G-CSF groups. The number of macrophages became small in each of the G-CSF and saline groups (Figure 3). However, it was significantly lower in the G-CSF group than the saline group.

Risk Area, Necrotic Area, Granulation Tissue Area, Scar Tissue Area, Collagen Area, Surviving Area, and Size of Cardiomyocytes

Among the 2-day, 7-day, 14-day, and 3-month groups, there were no significant differences of LV weights, LV areas, and nonrisk areas in any of the G-CSF and saline groups (Figure 4). The risk areas were significantly reduced in each of the G-CSF and saline groups at 14 days and 3 months after MI, compared with those at 2 days after MI, although the risk areas at 2 days after MI were similar between the G-CSF and saline groups (Figure 4).

The MI areas at 2 days after MI (necrotic tissue areas) were similar between the G-CSF and saline groups. However, they were reduced slightly in the saline groups and markedly in the G-CSF groups at 7 days (necrotic areas+granulation areas), 14 days (granulation areas), and 3 months (scar areas) after MI (Figure 4). The differences between the G-CSF and saline groups were significant. The necrotic areas, which were similar between the G-CSF and saline groups at 2 days after MI, were reduced moderately in the saline group and markedly in the G-CSF group at 7 days after MI (Figure 4). The difference between the 2 groups was significant. The granulation areas at 7 and 14 days after MI were significantly smaller in the G-CSF groups than the saline groups (Figure 4). In addition, the scar areas at 3 months after MI were significantly smaller in the G-CSF group than the saline group (Figure 4). Collagen areas with positive Sirius red

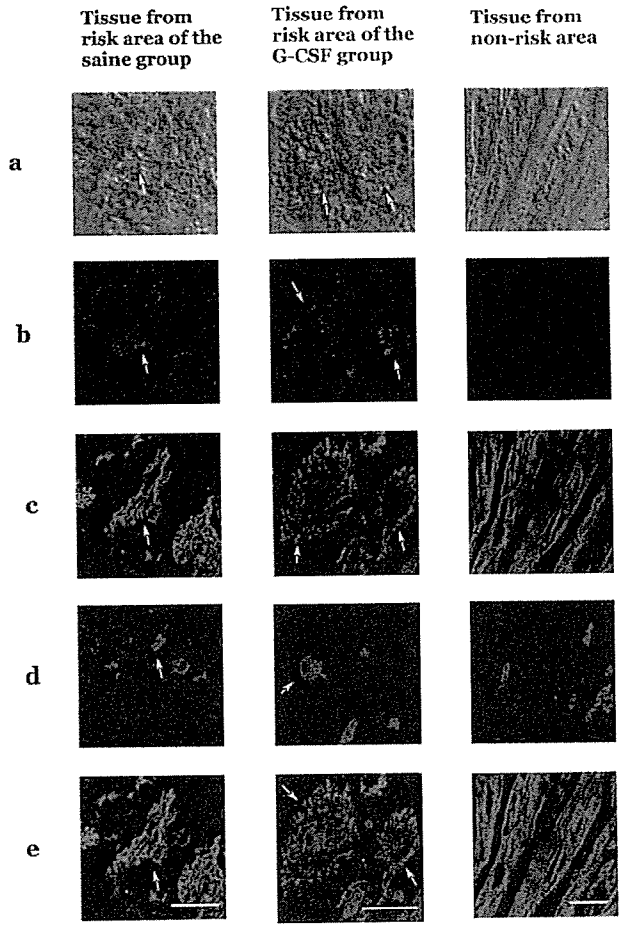

Figure 6. Confocal microscopic findings 14 days after infarction. Cells with positive DiI, an indicator of BM-derived cells, and positive troponin I, an indicator of cardiomyocytes, are observed in both saline and G-CSF groups. Note greater number in G-CSF group.

staining were significantly smaller in the G-CSF groups than the saline groups at 14 days and 3 months after MI (Figure 5).

The surviving areas of the saline groups within the risk areas were similar at 2 days, 7 days, 14 days, and 3 months after MI (Figure 4). However, those of the G-CSF groups were significantly larger at 14 days and 3 months after MI compared with that at 2 days after MI. The difference between the G-CSF and saline groups was significant at 14 days and 3 months after MI.

The transverse size of cardiomyocytes in the border zone between the surviving and infarct areas was significantly greater than that of the nonrisk areas in the G-CSF and saline groups even 2 days after MI (Figure 5). However, the sizes were similar between the saline and G-CSF groups and among 2 days, 7 days, 14 days, and 3 months after MI (Figure 5).

DiI-Labeled Cells

Confocal microscopy revealed the DiI-labeled cells with positive troponin I, a specific marker of cardiomyocytes (Figure 6); CD31, a marker of endothelial cells; or α-smooth muscle actin in the myocardial tissues obtained from the risk area but not in the tissues from the nonrisk area in the saline and G-CSF groups 14 days after MI (Figure 7). The DiI-labeled cells with positive α-smooth muscle actin were seen in the small vessels, indicating smooth muscle cells, and in the extravascular areas, indicating myofibroblasts (Figure 7). The percentages of DiI-labeled cells in troponin I–positive cells were significantly increased in the G-CSF group ($0.13\pm0.03\%$ versus $0.05\pm0.02\%$ of the saline group). The percentages of DiI-labeled cells in CD31-positive cells and α-smooth muscle actin–positive cells were significantly increased in the G-CSF group (6.9 ± 1.7 and $5.4\pm1.6\%$ versus 3.3 ± 1.1 and $1.7\pm0.7\%$ of the saline group, respectively).

In the BM of iliac crests, DiI-positive cells with nuclei showed a scattered distribution (Figure 7), suggesting the reconstruction of the injected BM cells.

MMP Expression

MMP 1 was significantly increased in the risk area of the saline and G-CSF groups and in the nonrisk area of the G-CSF group compared with that of the sham group (Figure 8). It was greatest in the risk area of the G-CSF group. MMP 9 was significantly increased in the risk area and nonrisk area of the G-CSF group.

Discussion

Acceleration of the Postinfarction Healing Process by G-CSF

The present study revealed that necrotic tissue areas as acute MI size were similar in the G-CSF and saline groups 2 days after MI but were smaller in the G-CSF group 7 days after MI. At 2 days after MI, the numbers of infiltrated neutrophils and macrophages in the acute MI areas, which have strong phagocytosis, were definitely increased in the G-CSF group. Therefore, the prompt absorption of necrotic tissues by G-CSF may be related to the enhanced mobilization of neutrophils and macrophages from BM.

Granulation, scar, and collagen areas were smaller in the G-CSF groups than the saline groups. MMP 1, a collagenase, and MMP 9, a gelatinase, were overexpressed in the G-CSF groups. This is similar to previous findings that G-CSF enhances the MMP family in cancer and blood cells.[12,13] Therefore, the reducing effect of collagen by G-CSF may be related to overexpression of the MMP family. Many studies showed that G-CSF improves the healing process of skin wounds such as doxorubicin-induced skin necrosis and burn injury of animal models and infected ulcers of the foot in patients with diabetes mellitus.[7–9] Improvement of immunocompromised states by G-CSF has been suggested.[8] This is supported by the lower level of macrophages at the subacute and chronic stages in the present study. Thus, post-MI G-CSF treatment accelerates the healing process of MI wounds.

Regeneration of Myocardial Tissues by G-CSF

At present, progenitor cells of cardiomyocytes, in addition to those of endothelial cells and smooth muscle cells, may be present in the myocardium itself, as in the BM. To define whether MI alone and G-CSF can mobilize BM-derived progenitor cells from BM into the heart, BM mononuclear cells labeled with DiI were returned into BM of the iliac

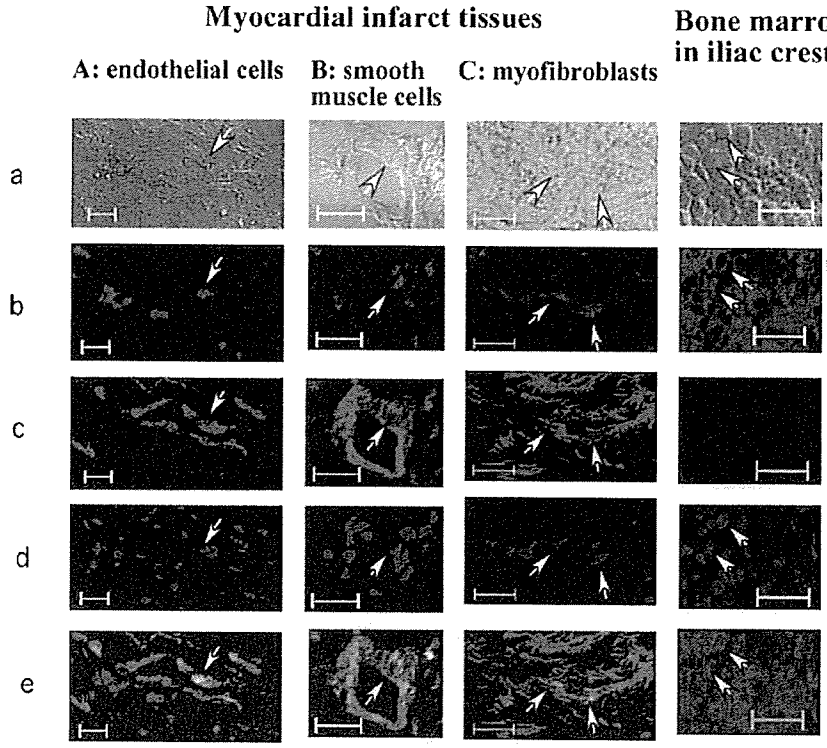

Figure 7. Confocal microscopic findings of saline group 14 days after infarction. Note presence of BM (BM)-derived endothelial cells, smooth muscle cells and myofibroblasts shown by arrows. Also note reconstruction of BM cells injected into iliac crest.

crests. DiI-positive and troponin I–, CD31-, or α-smooth muscle actin–positive cells, suggesting the transdifferentiated cardiomyocytes, endothelial cells, or smooth muscle cells (or myofibroblasts), respectively, were seen in the risk areas of the saline and G-CSF groups. The percentages were increased by G-CSF treatment. Thus, MI itself may induce regeneration of myocardial cells via mobilization of BM stem cells, and G-CSF may enhance the process.

However, several recent in vivo studies reported the presence of fusion between cardiomyocytes and BM progenitor cells.[14] In the present study, we cannot deny its possibility. In addition, the number of regenerated cells mobilized from the BM of the whole body is unknown because of the methodological limitations of the present study. However, surviving myocardial tissue areas within the risk areas in the G-CSF groups were increased 14 days and 3 months after MI. The transverse size of cardiomyocytes within the risk areas was similar between the G-CSF and saline groups. Death of cardiomyocytes is determined within several hours after reperfusion. In the present study, the first G-CSF injection was performed 24 hours after reperfusion, and acute infarct size at 2 days after reperfusion was similar between the G-CSF and saline groups. Therefore, it is considered that cell fusion caused by G-CSF therapy may occur between the BM cells and surviving cardiomyocytes in the risk areas, but it could not rescue the cardiomyocyte death in the present study. This suggests that an increase of surviving myocardial tissue areas by G-CSF is a result of regeneration of myocardial tissues, including cardiomyocytes. A part of the cells in the regenerated myocardial tissues may originate from BM progenitor cells. There is a possibility that hematopoietic stem cells are involved in the progenitor cells that were responsible for myocardial regeneration, because G-CSF generally mobilizes hematopoietic stem cells.

Mechanism of Improvement of LV Remodeling and Function by G-CSF

First, the enhanced myocardial tissue regeneration would contribute to the beneficial effects as detailed previously.[6] Second, rapid absorption of necrotic tissues relating to the higher level of neutrophils and macrophages at the acute stage and improvement of chronic inflammation suggested by the lower level of macrophages at the subacute and chronic stages may contribute to the beneficial effects. Third, production of fibrosis after MI prevents structural fragility. Previous studies reported that a MMP family was increased in the postinfarction heart failure models with permanent occlusion and large infarction and that the inhibitors beneficially affected cardiac remodeling and function.[15,16] Thus, it is suggested that an increase in MMP has an aggravating effect on heart failure via collagen degradation. However, it is well known that the volume of reactive granulation and/or scar tissues after skin injury after burn, surgery, etc, frequently becomes excessive, and this is called hypertrophic scarring. The excessive extent of fibrosis without contractility or relaxation would accelerate cardiac remodeling and decrease cardiac function, as seen in ischemic or idiopathic dilated cardiomyopathy. In such cases, an increase in the MMP family may be one of the protective mechanisms via proteolysis of excessive collagen. In fact, this concept is supported by findings of several previous studies: an inhibition of MMP caused cardiac failure,[17] targeted deletion of MMP 9 attenuated LV remodeling and collagen accumulation via overexpression of MMP-2 and MMP-13,[18] and an increase in

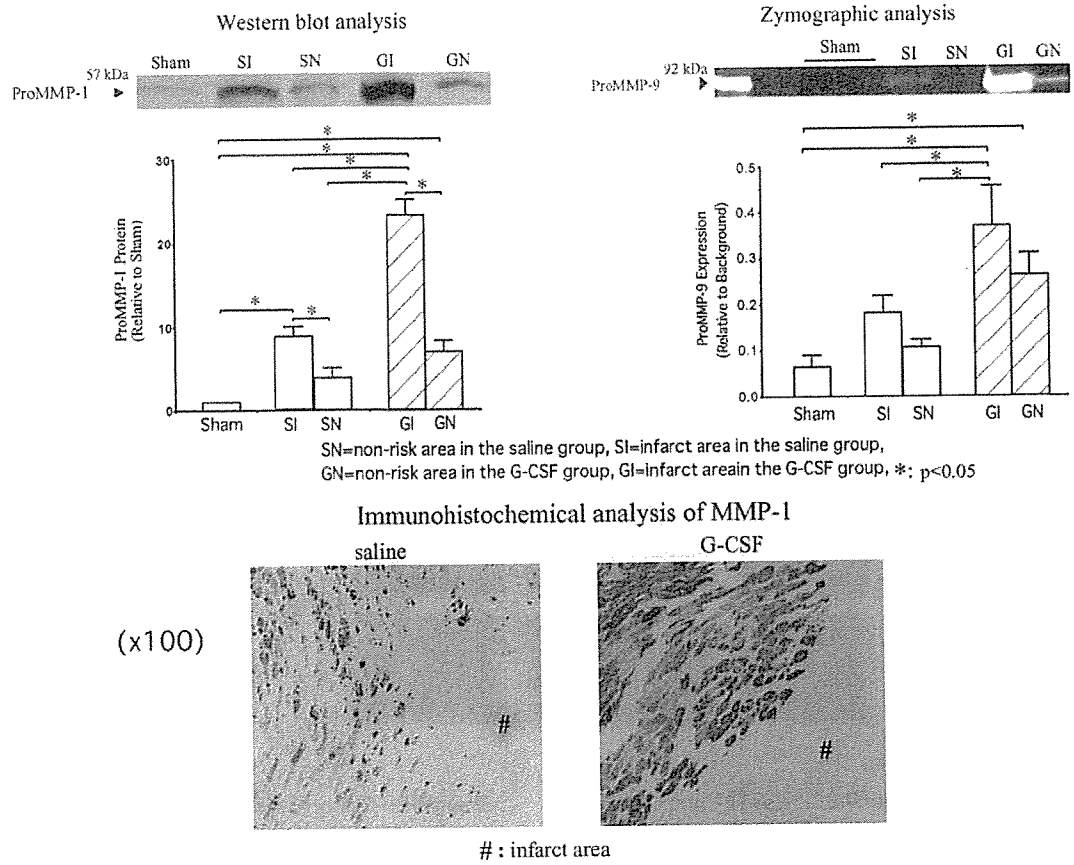

Figure 8. MMP 1 and 9 at 7 days after infarction. Note overexpression of MMP 1 and 9 in G-CSF group. MMP 1 was expressed in cardiomyocytes surrounding infarct area, and expression was greater in G-CSF group.

MMP-1 by hepatocyte growth factor was beneficial on post-MI heart failure via its anti-fibrotic action;[19] reduction of scar tissue and improvement of remodeling were observed simultaneously in myocardial regeneration therapy.[1,6] An adequate content of fibrosis may be different because of the various conditions of MI models, such as small or large MI, small or large amount of myocardial regeneration, and permanent or transient ischemia. Thus, in the present model with transient ischemia and nonlarge infarction, the beneficial effect of G-CSF relies on a higher number of migrated neutrophils/macrophages and upregulation of MMPs and increased participation of mobilized stem cells, which supports the concept of myocardial repair after infarction by Orlic et al.[6] Also, further investigation using MMP gene–defective mice or mice with blocking antibody would be warranted to define the precise role of MMP.

Clinical Implications

The standard therapy for human MI is reperfusion therapy, and our study showed the beneficial effect of G-CSF using a reperfusion model. The dose of G-CSF and the increased level in peripheral leukocytes were similar to those in a normal human donor for BM transplantation.[20] In addition to modification of the healing process and regeneration of myocardial tissues, this would offer the important suggestion of using the clinical application of G-CSF as a noninvasive therapy.

Conclusions

Both the acceleration of the healing process and myocardial regeneration play an important role in the beneficial effects of G-CSF.

Acknowledgments

This study was supported in part by Research Grants of Frontier Medicine (15209027, 15590732, and 14570700) from the Ministry of Education, Science, and Culture of Japan.

References

1. Orlic D, Kajstura J, Chimenti S, et al. Bone marrow cells regenerate infarcted myocardium. *Nature*. 2001;410:701–705.
2. Asahara T, Masuda H, Takahashi T, et al. Bone marrow origin of endothelial progenitor cells responsible for postnatal vasculogenesis in physiological and pathological neovascularization. *Circ Res*. 1999;85:221–228.
3. Wagers AJ, Sherwood RI, Christensen JL, et al. Little evidence for developmental plasticity of adult hematopoietic stem cells. *Science*. 2002;297:2256–2259.
4. Taylor DA, Hruban R, Rodriguez ER, et al. Cardiac chimerism as a mechanism for self-repair: does it happen and if so to what degree? *Circulation*. 2002;106:2–4.
5. Takemura G, Ohno M, Hayakawa Y, et al. Role of apoptosis in the disappearance of infiltrated and proliferated interstitial cells after myocardial infarction. *Circ Res*. 1998;82:1130–1138.
6. Orlic D, Kajstura J, Chimenti S, et al. Mobilized bone marrow cells repair the infarcted heart, improving function and survival. *Proc Natl Acad Sci USA*. 2001;98:10344–10349.
7. Vargel I, Erdem A, Ertoy D, et al. Effects of growth factors on doxorubicin-induced skin necrosis: documentation of histomorphological

alterations and early treatment by GM-CSF and G-CSF. *Ann Plastic Surg.* 2002;49:646–653.
8. Peter FW, Schuschke DA, Barker JH, et al. The effect of severe burn injury on proinflammatory cytokines and leukocyte behavior: its modulation with granulocyte colony stimulating factor. *Burns.* 1999;25:477–486.
9. Gough A, Clapperton M, Rolando N, et al. Randomised placebo-controlled trial of granulocyte-colony stimulating factor in diabetic foot infection. *Lancet.* 1997;350:855–859.
10. Minatoguchi S, Arai S, Uno Y, et al. Anti-diabetic drug, miglitol, markedly reduces myocardial infarct size in rabbits. *Br J Pharmacol.* 1999;128:1667–1672.
11. Kalka C, Masuda H, Takahashi T, et al. Transplantation of ex vivo expanded endothelial progenitor cells for therapeutic neovascularization. *Proc Natl Acad Sci U S A.* 2000;97:3422–3429.
12. Sugimoto C, Fujieda S, Sunaga H, et al. Granulocyte colony-stimulating factor (G-CSF)-mediated signaling regulates type IV collagenase activity in head and neck cancer cells. *Int J Cancer.* 2001;93:42–46.
13. Carstanjen D, Ulbricht N, Lacone A, et al. Matrix metalloproteinase-9 (gelatinase B) is elevated during mobilization of peripheral blood progenitor cells by G-CSF. *Transfusion.* 2002;42:588–596.
14. Alvarez-Dolado M, Pardal R, Garcia-Verdugo JM, et al. Fusion of bone-marrow-derived cells with Purkinje neurons, cardiomyocytes and hepatocytes. *Nature.* 2003;425:968–973.
15. Spinale FG. Matrix metalloproteinases: regulation and dysregulation on the failing heart. *Circ Res.* 2002;90:520–530.
16. Creemers EEJM, Cleutjens JPM, Smits JFM, et al. Matrix metalloproteinase inhibition after myocardial infarction: a new approach to prevent heart failure? *Circ Res.* 2001;89:201–210.
17. Heymans S, Luttun A, Nuyens D, et al. Inhibition of plasminogen activators or matrix metalloproteinases prevents cardiac rupture but impairs therapeutic angiogenesis and causes cardiac failure. *Nat Med.* 1999;5:1135–1142.
18. Ducharme A, Frantz S, Aikawa M, et al. Targeted deletion of matrix metalloproteinase-9 attenuates left ventricular enlargement and collagen accumulation after experimental myocardial infarction. *J Clin Invest.* 2000;106:55–62.
19. Taniyama Y, Morishita R, Nakagami H, et al. Potential contribution of a novel antifibrotic factor, hepatocyte growth factor, to prevention of myocardial fibrosis by angiotensin II blockade in cardiomyopathic hamsters. *Circulation.* 2000;102:246–252.
20. Kroger N, Renges H, Kruger W, et al. A randomized comparison of once versus twice daily recombinant human granulocyte colony-stimulating factor (Filgrastim) for stem cell mobilization in healthy donors for allogeneic transplantation. *Br J Haematol.* 2000;111:761–765.

Journal of the American College of Cardiology
© 2004 by the American College of Cardiology Foundation
Published by Elsevier Inc.

Vol. 43, No. 10, 2004
ISSN 0735-1097/04/$30.00
doi:10.1016/j.jacc.2004.01.034

Powerful and Controllable Angiogenesis by Using Gene-Modified Cells Expressing Human Hepatocyte Growth Factor and Thymidine Kinase

Yasuyo Hisaka, MS,* Masaki Ieda, MD,† Toshikazu Nakamura, PHD,‡ Ken-ichiro Kosai, MD, PHD,§ Satoshi Ogawa, MD, PHD,† Keiichi Fukuda, MD, PHD*†

Tokyo, Osaka, and Fukuoka, Japan

OBJECTIVES This study investigated the possibility of achieving angiogenesis by using gene-modified cells as a vector.

BACKGROUND Although gene therapy for peripheral circulation disorders has been studied intensively, the plasmid or viral vectors have been associated with several disadvantages, including unreliable transfection and uncontrollable gene expression.

METHODS Human hepatocyte growth factor (hHGF) and thymidine kinase (TK) expression plasmids were serially transfected into NIH3T3 cells, and permanent transfectants were selected (NIH3T3 + hHGF + TK). Unilateral hindlimb ischemia was surgically induced in BALB/c nude mice, and cells were transplanted into the thigh muscles. All effects were assessed at four weeks.

RESULTS The messenger ribonucleic acid expression and protein production of hHGF were confirmed. Assay of growth inhibition by ganciclovir revealed that the 50% (median) inhibitory concentration of NIH3T3 + hHGF + TK was 1,000 times lower than that of NIH3T3 + hHGF. The NIH3T3 + hHGF + TK group had a higher laser Doppler blood perfusion index, higher microvessel density, wider microvessel diameter, and lower rate of hindlimb necrosis, as compared with the plasmid- and adenovirus-mediated hHGF transfection groups or the NIH3T3 group. The newly developed microvessels were accompanied by smooth muscle cells, as well as endothelial cells, indicating that they were on the arteriolar or venular level. Laser Doppler monitoring showed that the rate of blood perfusion could be controlled by oral administration of ganciclovir. The transplanted cells completely disappeared in response to ganciclovir administration for four weeks.

CONCLUSIONS Gene-modified cell transplantation therapy induced strong angiogenesis and collateral vessel formation that could be controlled externally with ganciclovir. (J Am Coll Cardiol 2004;43: 1915–22) © 2004 by the American College of Cardiology Foundation

Growth factors isolated recently, including vascular endothelial cell growth factor, fibroblast growth factor, angiopoietin, and hepatocyte growth factor (HGF), have been found to induce strong angiogenesis (1–5). A number of studies have reported induction of angiogenesis and collateral vessel formation by gene therapy with these factors in both animal experiments and clinical trials. Plasmid or viral vectors have been used in these therapies (2,6,7), but the adenovirus vector entails some serious problems, such as allergic reactions or difficulty with repeated treatment, despite sufficiently high transfection efficiency. Moreover, although plasmid vectors have recently been used in clinical settings, have not been associated with allergic reactions, and could be used repeatedly, their transfection efficiency has been low and has varied with the tissues injected or the patient. These gene delivery methods have the common drawbacks of not being able to choose the target cells and to selectively eliminate the transfected cells once they acquire the character of abnormal growth. Thus, new methods that would provide ideal gene delivery systems have long been awaited.

Regeneration therapy has recently been performed in many tissues and organs. Various types of cells regenerate from embryonic or adult stem cells, and these cells would be transplanted into patients. Rapid and sufficient establishment of angiogenesis and collateral vessel formation to promote the survival and function of the transplanted cells are especially important in terms of blood supply. We investigated regeneration of cardiomyocytes from adult stem cells and concluded that blood vessel formation into transplanted cells is crucial to their survival (8). Because angiogenic gene therapy with plasmid vectors has been insufficient to induce the rapid and powerful angiogenesis required for transplantation of the regenerated cells, a new method has been needed to address this problem.

In the present study, NIH3T3 cells were permanently transfected with a novel angiogenic human HGF (hHGF) and thymidine kinase (TK) of herpes simplex gene and then used as a gene therapy vector. Their effect on blood flow,

From the *Institute for Advanced Cardiac Therapeutics, †Cardiopulmonary Division, Department of Medicine, Keio University School of Medicine, Tokyo; ‡Division of Molecular Regenerative Medicine, Course of Advanced Medicine, Osaka University Graduate School of Medicine, Osaka; and the §Cognitive and Molecular Research Institute of Brain Disease, Kurume University School of Medicine, Fukuoka, Japan. This study was supported in part by research grants from the Ministry of Education, Science and Culture, Japan, and by Health Science Research Grants for Advanced Medical Technology from the Ministry of Welfare, Japan.

Manuscript received June 28, 2003; revised manuscript received December 10, 2003, accepted January 5, 2004.

JACC Vol. 43, No. 10, 2004
May 19, 2004:1915–22

Abbreviations and Acronyms

DMEM	= Dulbecco's modified Eagle's medium
EGFP	= enhanced green fluorescent protein
ELISA	= enzyme-linked immunosorbent assay
hHGF	= human hepatocyte growth factor
IC_{50}	= 50% (median) inhibitory concentration
LDPI	= laser Doppler perfusion image
RT-PCR	= reverse transcription-polymerase chain reaction
SMA	= smooth muscle actin
TK	= thymidine kinase
vWF	= von Willebrand factor

angiogenesis, and collateral formation was investigated in a murine ischemic hindlimb model (9–11). In this paper, we report that gene-modified cells expressing hHGF and TK induced strong angiogenesis and collateral vessel formation, and that they were easily controlled externally with ganciclovir.

METHODS

Cell culture. The NIH3T3 cells were cultured in Dulbecco's modified Eagle's medium (DMEM), supplemented with 10% fetal bovine serum and penicillin (100 μg/ml), streptomycin (250 ng/ml), and amphotericin B (85 μg/ml).

Stable transfection of hHGF and TK genes. The complementary deoxyribonucleic acid (cDNA) of the hHGF and TK genes was inserted into the pUC-SRα and pGK expression vector plasmids, respectively (10–13). pPUR and pcDNA3.1/Hygro(+) are selection plasmids that confer puromycin resistance and hygromycin resistance, respectively. After co-transfection of pUC-SRα/hHGF and pPUR into the NIH3T3 cells, using the Effectene Reagent (QIAGEN GmbH, Hilden, Germany), the puromycin-nonresistant cells were removed with puromycin (3 μg/ml), and the hHGF-producing cells were clonally selected (NIH3T3 + hHGF). pGK/TK and pcDNA3.1/Hygro(+) plasmids were then similarly co-transfected into the NIH3T3 + hHGF cells; the hygromycin-nonresistant cells were removed with hygromycin (200 μg/ml); and both hHGF- and TK-producing cells were clonally selected (NIH3T3 + hHGF + TK).

Reverse transcription-polymerase chain reaction (RT-PCR). Expression of hHGF messenger ribonucleic acid was analyzed by RT-PCR using the primers that specifically detect human but not mouse HGF, as previously described (14).

Enzyme-linked immunosorbent assay (ELISA) for hHGF. Production of hHGF was determined by ELISA with anti-human–specific HGF monoclonal antibodies (Institute of Immunology, Tokyo, Japan) (6,15,16).

Ad.CA-hHGF. The adenoviral vector plasmid pAd.CA-hHGF, which is composed of a cytomegalovirus immediate early enhancer, a modified chicken beta-actin promoter, and hHGF cDNA, was constructed by the in vitro ligation method (17). The pAd.CA-hHGF plasmid was partially cut with *Pac*I and then transfected into 293 cells, followed by culture with 0.5% overlaid agarose-α-minimal essential medium (MEM) containing 5% horse serum for 10 to 15 days. Viral plaques, which had been confirmed by restriction enzyme analysis and ELISA for hHGF, were propagated in 293 cells, purified by $CsCl_2$ gradient ultracentrifugation twice, and desalted with a desalting column (18). Viral particles were calculated by means of optical density at 260 nm.

Murine model of hindlimb ischemia. All animal experiments were approved by the Animal Care and Use Committee of Keio University. After anesthetizing male BALB/c nude mice (eight weeks) with diethyl ether, the femoral artery was gently isolated, and the proximal portion was ligated with 7-0 silk ligatures (19,20).

Transplantation of continuously hHGF-producing NIH3T3 cells. The hindlimb ischemic mice (n = 192) were randomly classified into five groups. The control groups received 0.2 ml saline only (n = 14), 500 μg pUC-SRα/hHGF plasmids in 0.2 ml saline (n = 10), 10^9 particles Ad.CA-hHGF in 0.2 ml phosphate-buffered saline (n = 10), or NIH3T3 in 0.2 ml DMEM (n = 14). The experimental group received NIH3T3 + hHGF + TK in 0.2 ml DMEM (n = 144). All injections were given via a 27-gauge needle (21). The numbers of cells transplanted ranged from 10^4 to 10^7. They were injected into two different sites in the ischemic thigh (adductor) skeletal muscles on postoperative day 1. The direction of injection was parallel to the muscle fibers. Angiogenesis and collateral vessel formation were assessed at four weeks.

Laser Doppler blood perfusion analysis. The blood perfusion rate in the ischemic (left leg) and normal (right leg) hindlimb was measured with a laser Doppler perfusion image (LDPI) system (Moor Instruments), as described previously (20,22).

Histopathology. Frozen sections (4 μm) were cut from tissue specimens (23). Immunohistochemical staining for hHGF, endothelial cells, and alpha-smooth muscle actin (SMA) was carried out with anti-human HGF (R&D Systems Inc., Minneapolis, Minnesota), anti-human von Willebrand factor (vWF)/horseradish peroxidase (HRP), and anti-human SMA/HRP (Dakocytomation, Kyoto, Japan), respectively. Sections for staining and counterstaining were incubated with 3,3′-diaminobenzidine tetrahydrochloride and Mayer's hematoxylin solution, respectively. Elastica van Gieson staining was carried out by the standard method. Paraffin sections (3 μm) were cut from tissue specimens, and hematoxylin-eosin staining was carried out by the standard method.

Assay of growth inhibition by ganciclovir in vitro. After seeding cells on six-well plates (10^5 cells/well) and culturing for 24 h, they were exposed to ganciclovir in concentrations ranging from 0 to 10^{-3} g/ml for 72 h (24,25).

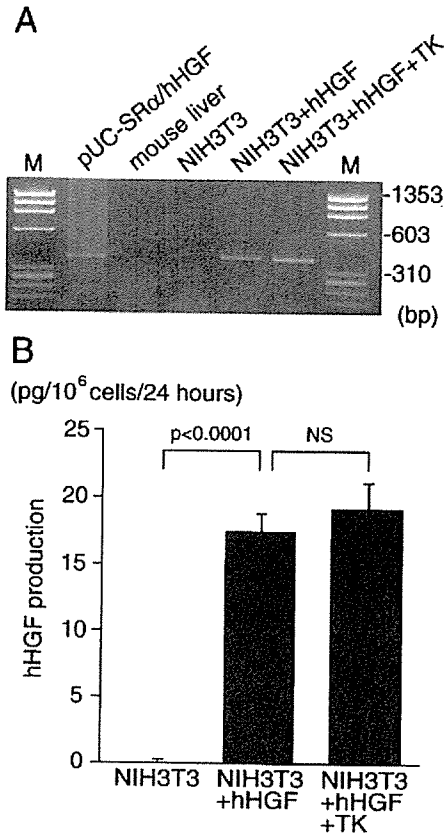

Figure 1. (A) Expression of human hepatocyte growth factor (hHGF) messenger ribonucleic acid in the hHGF-transfected NIH3T3 cells. The primer set of reverse transcription-polymerase chain reaction specifically detects hHGF but not mouse HGF. pUC-SRα/hHGF plasmid and mouse liver were used as a positive and negative control, respectively. M = the ΦX174-*Hae*III digest. (B) Production of hHGF protein. This ELISA system specifically detects only hHGF because of the lack of cross-reactivity by the antibodies. Data are expressed as hHGF concentrations adjusted for cell number. Both NIH3T3 + hHGF and NIH3T3 + hHGF + thymidine kinase (TK) groups expressed hHGF messenger ribonucleic acid and produced hHGF protein (n = 5).

Detection of ganciclovir-induced apoptosis with annexin V. Annexin V is an early apoptotic marker. The NIH3T3 + hHGF + TK group was exposed to 10^{-7} g/ml ganciclovir for 48 h, and the apoptotic cells were detected with an annexin V-enhanced green fluorescent protein (EGFP) apoptosis detection kit (Medical & Biological Labs Co. Ltd., Nagaya, Japan) (26).

Regulation of transplanted cell growth with ganciclovir in vivo. We investigated the dose-response relationship of growth inhibition by ganciclovir by transplanting NIH3T3 + hHGF + TK (10^7 cells) and administering ganciclovir two weeks later. The transplanted mice received different doses (0, 1, 10, 50, or 80 mg/kg per day) of ganciclovir orally once a day for four weeks.

Statistical analysis. The data were processed using StatView J-4.5 software. Results are reported as the mean value ± SE. Comparisons of values among all groups were performed by one-way analysis of variance. The Scheffe's *F* test was used to determine the level of significance. The probability level accepted for significance was $p < 0.05$.

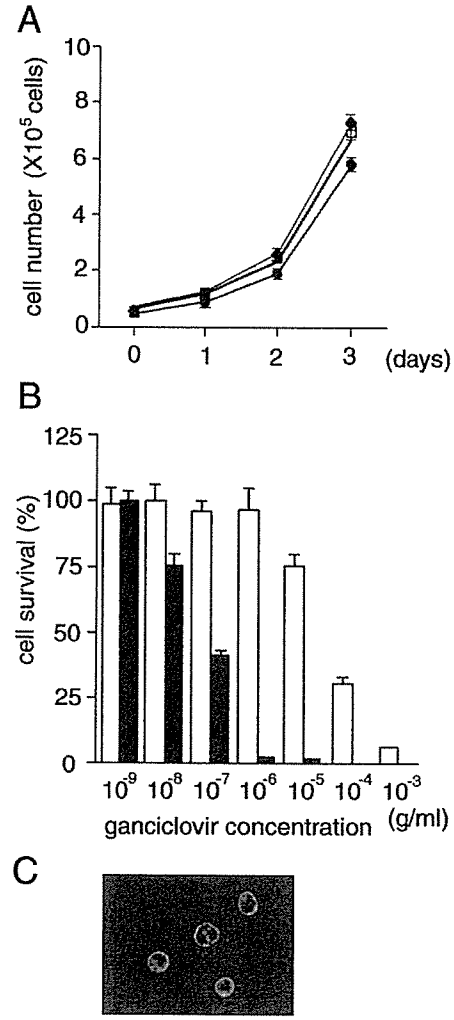

Figure 2. (A) Influence of hHGF and/or TK genes on cell growth in vitro. The growth rate of the hHGF-transfected NIH3T3 cells was slightly higher than that of the nontransfected cells, but TK had no effect on cell growth. (**circles** = NIH3T3; **diamonds** = NIH3T3 + hHGF; **squares** = NIH3T3 + hHGF + TK) (n = 3). (B) Growth-inhibitory effect of ganciclovir. The IC_{50} of ganciclovir for the NIH3T3 + hHGF + TK group (**solid bars**) was ~1,000 times lower than that for the NIH3T3 + hHGF group (**open bars**) (n = 5). (C) Apoptotic cells stained with annexin V-EGFP at the cell membrane after exposure to ganciclovir. Abbreviations as in Figure 1.

RESULTS

Permanently hHGF-transfected NIH3T3 cells produced hHGF protein. The NIH3T3 + hHGF cells were obtained after two weeks of exposure to puromycin, and NIH3T3 + hHGF + TK cells were obtained after two more weeks of exposure to hygromycin. We confirmed that both the NIH3T3 + hHGF and NIH3T3 + hHGF + TK groups expressed hHGF mRNA and then produced hHGF protein at a rate of 17.3 ± 1.4 and 19.1 ± 2.0 pg/10^6 cells per 24 h, respectively (Fig. 1).

Ganciclovir-inhibited cell growth and induced apoptotic cell death. It is well known that HGF regulates cell growth. To determine whether transfection of hHGF affects the growth of NIH3T3 cells, we counted the numbers

JACC Vol. 43, No. 10, 2004
May 19, 2004:1915–22

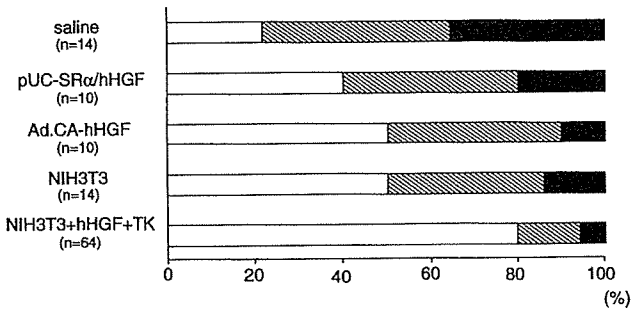

Figure 3. Frequency of necrosis in the ischemic hindlimbs. Severe hindlimb necrosis was significantly reduced in the NIH3T3 + hHGF + TK group. **Open areas** = negative necrosis; **lined areas** = necrosis on toes; **solid areas** = necrosis on foot. Abbreviations as in Figure 1.

of cells in vitro (Fig. 2A). The growth rate of the hHGF-transfected NIH3T3 cells seemed to increase slightly, but the increase was not significant on day 3. Transfection of the TK gene had no effect on their growth rate.

Next, we investigated the growth-inhibitory effect of ganciclovir on these cells (Fig. 2B). The IC_{50} of ganciclovir for the NIH3T3 + hHGF + TK group was ~1,000 times lower than that for the NIH3T3 + hHGF group. These findings confirmed that the TK plasmid genes had been effectively transfected, and that hardly any of the cells that expressed the TK gene survived exposure to ganciclovir at a concentration of 10^{-6} g/ml, which did not affect the control cells.

Enhanced green fluorescent protein fluorescence was detected at the membranes of NIH3T3 + hHGF + TK cells after ganciclovir exposure (Fig. 2C), indicating that cell death was attributable to apoptosis.

Human HGF-producing cell therapy augmented angiogenesis and collateral vessel formation. To evaluate whether transplantation of hHGF-producing cells improves the perfusion of ischemic hindlimbs, we first determined the rate of necrosis of the ischemic hindlimb. Necrosis was rated on a three-grade scale. The rate of necrosis of the foot and toes in the saline group was 35.7% and 42.9%, respectively. The rates in the pUC-SRα/hHGF group were 20% and 40%, respectively, and in the Ad.CA-hHGF group 10% and 40%, respectively. These therapeutic approaches were effective in comparison with the saline group, but they were not sufficient to fully prevent the necrosis. To further ameliorate limb necrosis, we examined angiogenic gene-modified cell transplantation therapy. The NIH3T3 (10^7 cells) group had rates of 14.3% and 35.7%, respectively, suggesting that the vector cell transplantation itself might improve perfusion of the ischemic limb to some extent. In contrast, the rates in the NIH3T3 + hHGF + TK (10^7 cells) group were 5.8% and 14.5%, respectively (Fig. 3). The rate of necrosis was surprisingly reduced in the NIH3T3 + hHGF + TK group, indicating that transplantation of hHGF-producing cells might be one of the most effective methods of improving limb ischemia.

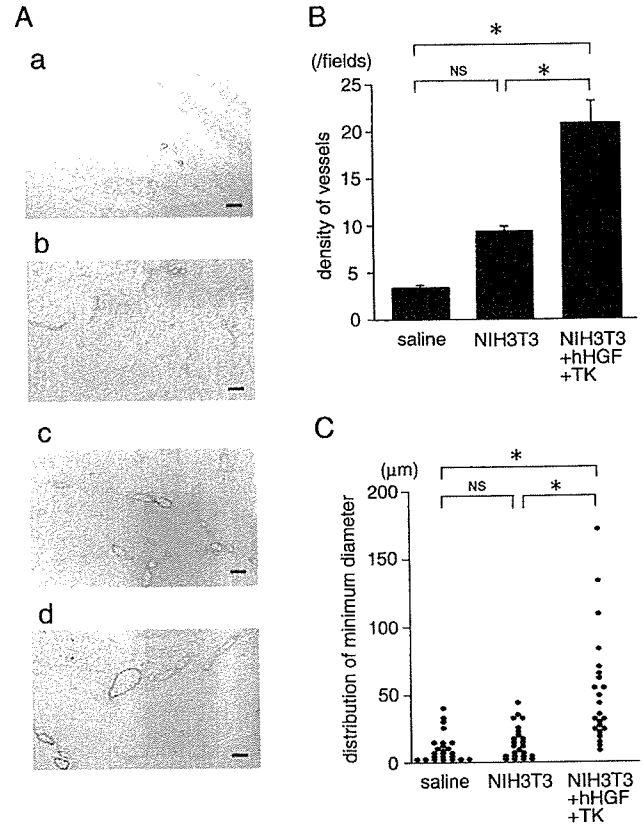

Figure 4. (A, panels a to d) Immunohistochemical staining for von Willebrand factor in the triceps muscle of the left calf revealed the presence of numerous vessels. Vessels were larger and more numerous in the NIH3T3 + hHGF + TK group **(panels c and d)** than in the saline **(panel a)** and NIH3T3 groups **(panel b). Scale bars** = 100 μm. **(B)** The number of vessels was determined by observation of 20 random fields from 10 mice (2 fields per mouse; *$p < 0.01$). **(C)** Distribution of the minimum diameters of the von Willebrand factor-positive vessels ($n = 25$; *$p < 0.0001$). Abbreviations as in Figure 1.

Vessel density and size. Immunostaining clearly revealed the presence of numerous vessels in the NIH3T3 + hHGF + TK group (Fig. 4A, panel c) and a lower number of vessels in the saline (Fig. 4A, panel a) and NIH3T3 (Fig. 4A, panel b) groups. Quantitative analysis revealed that the vessel density in the ischemic region was significantly higher (Fig. 4B), and the minimum diameter of the vWF-positive vessels was significantly greater (Figs. 4A, panel d, and 4C) in the NIH3T3 + hHGF + TK group.

Vessel maturation. Maturation of the vessels was investigated by staining three consecutive frozen sections of ischemic skeletal muscle. Amazingly, most of the vessels in the NIH3T3 + hHGF + TK group were vWF/α-SMA–double positive (Figs. 5A, panels a and b, and 5B). However, there was no increase in elastic fiber-positive cells, as compared with the saline and NIH3T3 groups (Figs. 5A, panel c, and 5B). These findings showed that NIH3T3 + hHGF + TK cell transplantation strongly induced angiogenesis not only at the capillary level but also at the microvessel (arteriole) level, and it caused angiogenesis at the large blood vessel level.

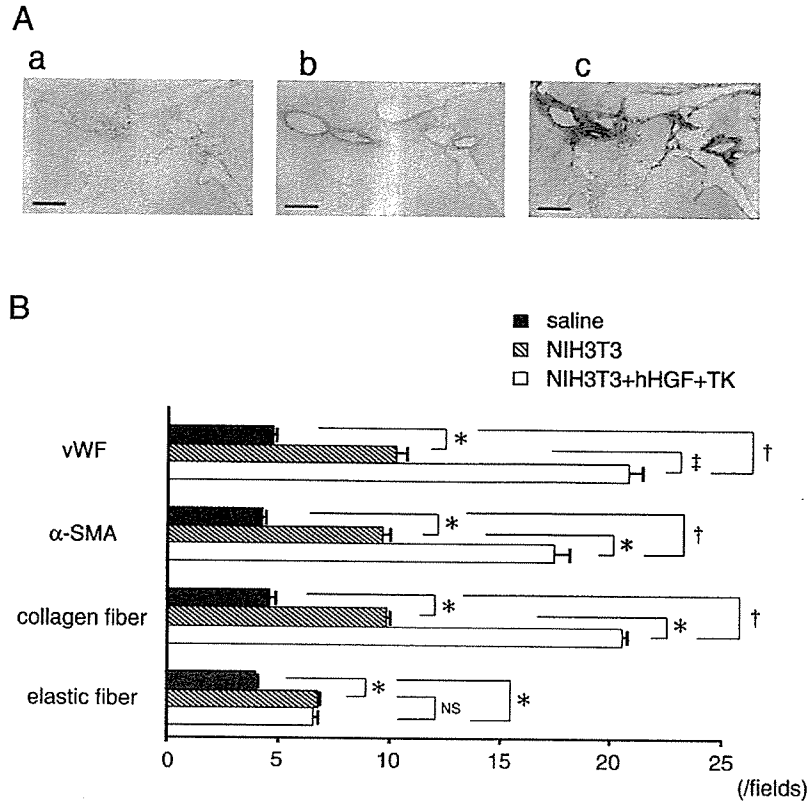

Figure 5. **(A, panels a to c)** Three consecutive frozen sections of NIH3T3 + hHGF + TK transplanted muscle. **(panel a)** Immunohistochemical staining for vWF and **(panel b)** α-smooth muscle actin (SMA) and **(panel c)** elastica van Gieson staining. **Scale bars** = 100 μm. **(B)** Maturation of vessels was compared by using three consecutive frozen sections. Most of the von Willebrand factor (vWF)-positive vessels in NIH3T3 + hHGF + TK transplanted mice also stained with α-SMA (n = 20; *p < 0.05, †p < 0.001, ‡p < 0.01). Abbreviations as in Figure 1.

Laser Doppler blood perfusion. The LDPI analysis was performed to study subcutaneous blood perfusion. Representative images are shown in Figure 6A, and quantitative analysis of blood perfusion is shown in Figure 6B. No blood perfusion was observed in the hindlimb immediately after femoral artery ligation (Fig. 6A, panel a). Perfusion of the proximal part of the thigh had recovered at four weeks in the saline and NIH3T3 groups, but perfusion distal to the heel joint had markedly decreased (Fig. 6A, panels b and c). In the NIH3T3 + hHGF + TK (10^4 cells) group, perfusion of the ischemic limb almost recovered to the control (nonischemic) level, but perfusion distal to the heel was slightly decreased compared with the control level (Fig. 6A, panel d). In the NIH3T3 + hHGF + TK (10^7 cells) group, perfusion of the ischemic limb was 118.1% (i.e., much greater than that in the control hindlimb) (Figs. 6A and 6B, panel e). To adjust the recovery of blood perfusion in the ischemic limb to the appropriate level, we transplanted NIH3T3 + hHGF + TK (10^7 cells), monitored the LDPI level, and began giving ganciclovir when blood perfusion reached the control level (two weeks). This method enabled us to adjust the blood perfusion rate in the ischemic limb to the same level as in the control limb (Figs. 6A and 6B, panel f).

When the NIH3T3 + hHGF + TK cells were transplanted into the normal nonischemic limb, the blood perfusion increased more than that in the control limb. Up to six weeks after transplantation, no evidence of angiosarcoma or hypervascular tumor was observed in the transplanted limb or other parts of the body (data not shown).

In vivo production of HGF protein. Immunohistochemical staining demonstrated the production of hHGF protein in transplanted NIH3T3 + hHGF + TK cells, but not in transplanted NIH3T3 cells (Fig. 7A).

Cell regulation with ganciclovir and TK. Figure 7B shows a quantitative analysis of the inhibitory effect of ganciclovir on blood perfusion. At a concentration of 50 mg/kg/day of ganciclovir, the blood perfusion was adjusted in the ischemic limb to the same level as in the control limb, and no significant side effects were produced. Histologic examination revealed the natural history of the transplanted cells (Fig. 7C, panels a to c). The transplanted cells formed a mass between the skeletal muscles, which gradually increased in size but did not infiltrate into the skeletal muscle. Two weeks after transplantation of the NIH3T3 + hHGF + TK cells, we began giving ganciclovir orally every day for two to four weeks and then examined tissue samples (Fig. 7C, panels d to f). The NIH3T3 + hHGF + TK cells gradually underwent apoptosis, and by four weeks, no transplanted cells could be detected. The surrounding muscle cells and the generated vessels were unaffected by ganciclovir.

JACC Vol. 43, No. 10, 2004
May 19, 2004:1915-22

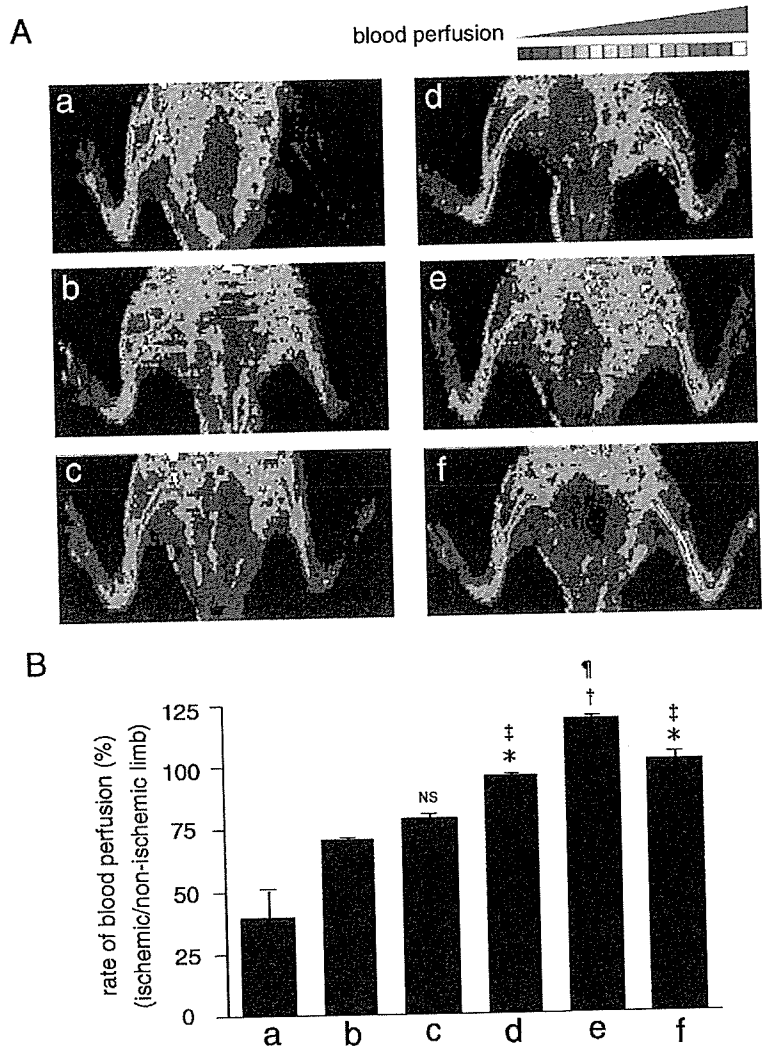

Figure 6. (A) Representative laser Doppler perfusion images. (B) Quantitative analysis of the rate of blood perfusion of the ischemic/nonischemic limb. **Panel a** = Control mouse on postoperative day 1; **panels b to f** = four weeks after treatment (**panel b** = saline injection; **panel c** = NIH3T3 transplantation [10^7 cells]; **panel d** = NIH3T3 + hHGF + TK transplantation [10^4 cells]; **panel e** = NIH3T3 + hHGF + TK transplantation [10^7 cells]; **panel f** = beginning two weeks after transplantation of NIH3T3 + hHGF + TK (10^7 cells), ganciclovir (50 mg/kg/day) was administered orally for four weeks. Oral ganciclovir administration adjusted the blood perfusion rate of the ischemic limb to the same level as that of the nonischemic limb (eight mice/group). *$p < 0.01$, †$p < 0.001$ vs. saline, ‡$p < 0.05$, ¶$p < 0.01$ versus NIH3T3. Abbreviations as in Figure 1.

DISCUSSION

In this study, we assessed angiogenic gene-modified cell transplantation therapy with fibroblasts permanently transfected with hHGF and TK genes in a murine hindlimb ischemia model. This therapy had the following merits: 1) it induced angiogenesis and collateral vessel formation more effectively than with plasmid and viral vectors. 2) The combination of TK and ganciclovir allowed the angiogenesis to be adjusted by monitoring LDPI. 3) This therapy could be stopped at any time desired for any reason. 4) There was no possibility of the hHGF gene being expressed in nontarget organs or nontarget cells as a result of leakage or dispersion of the vectors. If the plasmid vector was integrated into the genome and neoplastic transformation occurred, it would be difficult to control cell growth. 5) The angiogenic effect can be easily predicted, because the transfection efficiency of the gene is always 100%. 6) The cell vector will be much more effective in patients who require rapid angiogenesis, because plasmid or viral vectors require a week for maximal expression, and the duration of maximal expression is short.

Angiogenic gene-modified cell transplantation therapy has several drawbacks. One is that once the cells are transplanted into patients, their growth cannot be controlled. To solve this problem, we double-transfected the cells with the TK gene, and the results confirmed that permanently transfected cells could be killed with ganciclovir after the establishment of angiogenesis and collateral vessel formation. The finding that the IC_{50} of ganciclovir for the TK-transfected cells was 1,000 times lower than that in the nontransfected cells indicated that this system might be capable of being used in clinical settings.

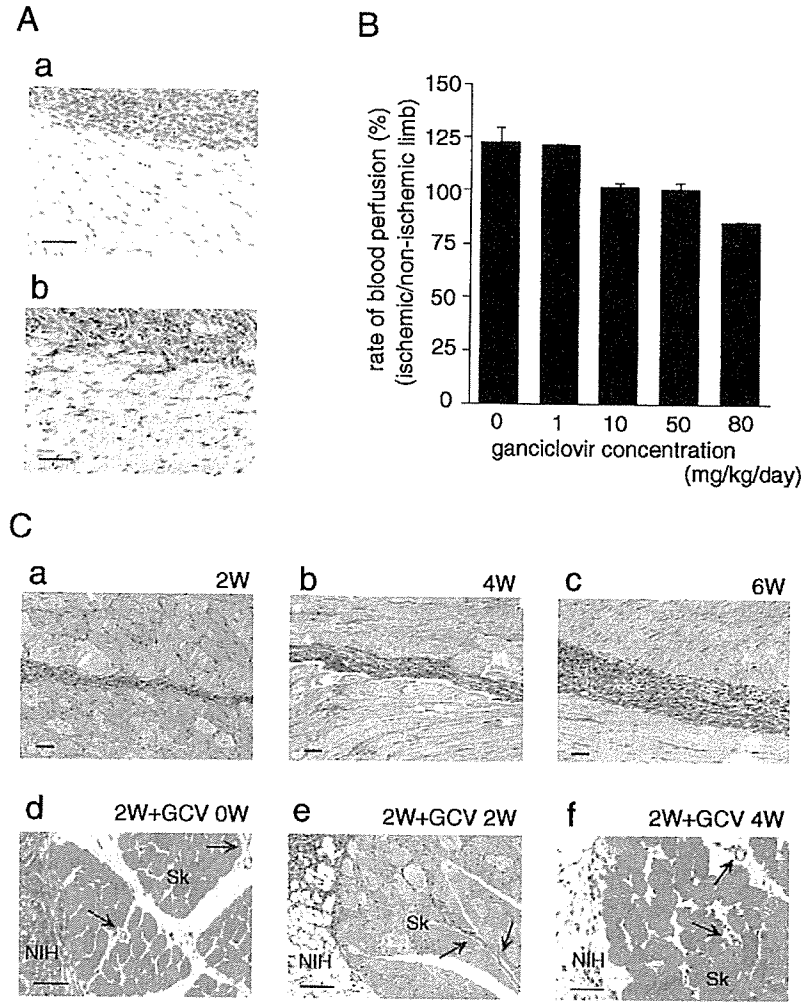

Figure 7. **(A)** Immunohistochemical staining for hHGF in transplanted NIH3T3 cells **(panel a)** and NIH3T3 + hHGF + TK cells **(panel b)** in the skeletal muscle. **Scale bars** = 50 μm. **(B)** The NIH3T3 + hHGF + TK (10^7) cells were transplanted, and two weeks later, various concentrations of ganciclovir were administered for another four weeks. **(C)** Hematoxylin-eosin staining. **(Panels a to c)** The natural history of the transplanted NIH3T3 + hHGF + TK (10^7) cells is shown. **(Panels d to f)** Beginning two weeks after transplantation, ganciclovir (50 mg/kg/day) was administered orally for two to four weeks. The cells had completely disappeared after four weeks of ganciclovir treatment. **Arrows** indicate the microvessels. **Scale bars** = 100 μm. Abbreviations as in Figure 1.

We used NIH3T3, a fibroblast line derived from fetal NIH/Swiss mice, for the following reasons: 1) the transfection efficiency of the plasmid is high; and 2) their growth rate is relatively high in vitro, making it easy to expand the cells. However, their growth rate in vivo is not as high as that of carcinoma cell lines, probably because NIH3T3 cells have a mechanism of growth inhibition by cell-cell contact. To apply this method in clinical medicine, the selection of a human cell line will be requried. Considering the time and cost for preparation of the cells, an autograft might require a long time and be expensive. It took at least two months to prepare the hHGF– and TK–double-transfected cells, and a number of additional experiments were needed to confirm their effectiveness and safety. We think that allograft cells should be used to prepare gene-modified cells. In view of the time, cost, effectiveness, and safety of the cells, allografts would be much better than autografts.

Regenerative medicine has recently been the subject of investigations in many fields, and a number of regenerative cells have been established. The authors have reported that regenerative cardiomyocytes can be generated from marrow mesenchymal stem cells, and transplantation of the regenerated cells will be examined in various organs. One of the reasons why we are considering angiogenic gene-modified cell transplantation therapy is the need for a rapid blood supply to the transplanted cells. To achieve that goal, we can co-transplant target organs with these gene-modified cells in combination with the regenerated cells. Once the blood supply has become established, the angiogenic cells are no longer needed, and they can be eliminated by ganciclovir.

Bone marrow mononuclear cells have recently been used to induce angiogenesis as a means of treating arteriosclerosis obliterans (27). Although bone marrow mononuclear cells contain endothelial cells, the population of endothelial progenitor cells is <1%. The effectiveness of this therapy may be explained not only by the presence of endothelial

JACC Vol. 43, No. 10, 2004
May 19, 2004:1915–22

progenitor cells but also by the fact that bone marrow mononuclear cells produce various cytokines and angiogenic growth factors. The advantage of angiogenic therapy with bone marrow mononuclear cell autografts is that the cells do not undergo immunorejection. The drawback of this therapy is that the cells may contain a variety of types of cells, such as osteogenic or chondrogenic stem cells, or induce inflammation by secreting cytokines. Using angiogenic gene-modified cells avoids the problem of transplanting different types of cells; however, the efficiency and safety of this procedure needs to be fully investigated before clinical application can become a reality.

Acknowledgments

The authors gratefully acknowledge Kensuke Kimura, MD, Isao Shibuya, PhD, and Haruko Kawaguchi, MS, for their kind assistance and helpful discussions.

Reprint requests and correspondence: Dr. Keiichi Fukuda, Institute for Advanced Cardiac Therapeutics, Keio University School of Medicine, 35 Shinanomachi, Shinjuku-ku, Tokyo 160-8582, Japan. E-mail: kfukuda@sc.itc.keio.ac.jp.

REFERENCES

1. Isner JM, Pieczek A, Schainfeld R, et al. Clinical evidence of angiogenesis after arterial gene transfer of phVEGF165 in patient with ischaemic limb. Lancet 1996;348:370–4.
2. Yukawa H, Takahashi JC, Miyatake SI, et al. Adenoviral gene transfer of basic fibroblast growth factor promotes angiogenesis in rat brain. Gene Ther 2000;7:942–9.
3. Suri C, McClain J, Thurston G, et al. Increased vascularization in mice overexpressing angiopoietin-1. Science 1998;282:468–71.
4. Morishita R, Nakamura S, Hayashi S, et al. Therapeutic angiogenesis induced by human recombinant hepatocyte growth factor in rabbit hind limb ischemia model as cytokine supplement therapy. Hypertension 1999;33:1379–84.
5. Carmeliet P. Mechanisms of angiogenesis and arteriogenesis. Nat Med 2000;6:389–95.
6. Hayashi S, Morishita R, Nakamura S, et al. Potential role of hepatocyte growth factor, a novel angiogenic growth factor, in peripheral arterial disease: downregulation of HGF in response to hypoxia in vascular cells. Circulation 1999;100 Suppl II:II301–8.
7. Byun J, Heard JM, Huh JE, et al. Efficient expression of the vascular endothelial growth factor gene in vitro and in vivo, using an adeno-associated virus vector. J Mol Cell Cardiol 2001;33:295–305.
8. Makino S, Fukuda K, Miyoshi S, et al. Cardiomyocytes can be generated from marrow stromal cells in vitro. J Clin Invest 1999;103:697–705.
9. Jainchill JL, Aaronson SA, Todaro GJ. Murine sarcoma and leukemia viruses: assay using clonal lines of contact-inhibited mouse cells. J Virol 1969;4:549–53.
10. Nakamura T, Nishizawa T, Hagiya M, et al. Molecular cloning and expression of human hepatocyte growth factor. Nature 1989;342:440–3.
11. McKnight SL. The nucleotide sequence and transcript map of the herpes simplex virus thymidine kinase gene. Nucleic Acids Res 1980;8:5949–64.
12. Hayashi S, Morishita R, Higaki J, et al. Autocrine-paracrine effects of overexpression of hepatocyte growth factor gene on growth of endothelial cells. Biochem Biophys Res Commun 1996;220:539–45.
13. Adra CN, Boer PH, McBurney MW. Cloning and expression of the mouse pgk-1 gene and the nucleotide sequence of its promoter. Gene 1987;60:65–74.
14. Ueda H, Sawa Y, Matsumoto K, et al. Gene transfection of hepatocyte growth factor attenuates reperfusion injury in the heart. Ann Thorac Surg 1999;67:1726–31.
15. Nakamura Y, Morishita R, Higaki J, et al. Expression of local hepatocyte growth factor system in vascular tissues. Biochem Biophys Res Commun 1995;215:483–8.
16. Yamada A, Matsumoto K, Iwanari H, et al. Rapid and sensitive enzyme-linked immunosorbent assay for measurement of HGF in rat and human tissues. Biomed Res 1995;16:105–14.
17. Mizuguchi H, Kay MA. A simple method for constructing E1- and E1/E4-deleted recombinant adenoviral vectors. Hum Gene Ther 1999;10:2013–7.
18. Chen SH, Chen XH, Wang Y, et al. Combination gene therapy for liver metastasis of colon carcinoma in vivo. Proc Natl Acad Sci USA 1995;92:2577–81.
19. Couffinhal T, Silver M, Zheng LP, Kearney M, Witzenbichler B, Isner JM. Mouse model of angiogenesis. Am J Pathol 1998;152:1667–79.
20. Murohara T, Asahara T, Silver M, et al. Nitric oxide synthase modulates angiogenesis in response to tissue ischemia. J Clin Invest 1998;101:2567–78.
21. Morishita R, Sakaki M, Yamamoto K, et al. Impairment of collateral formation in lipoprotein(a) transgenic mice: therapeutic angiogenesis induced by human hepatocyte growth factor gene. Circulation 2002;105:1491–6.
22. Shintani S, Murohara T, Ikeda H, et al. Augmentation of postnatal neovascularization with autologous bone marrow transplantation. Circulation 2001;103:897–903.
23. Takeshita S, Zheng LP, Brogi E, et al. Therapeutic angiogenesis: a single intraarterial bolus of vascular endothelial growth factor augments revascularization in a rabbit ischemic hind limb model. J Clin Invest 1994;93:662–70.
24. Smee DF, Martin JC, Verheyden JP, Matthews TR. Anti-herpesvirus activity of the acyclic nucleoside 9-(1,3-dihydroxy-2-propoxymethyl) guanine. Antimicrob Agents Chemother 1983;23:676–82.
25. Cho HS, Park YN, Lyu CJ, et al. Effects of retroviral-mediated herpes simplex virus thymidine kinase gene transfer to murine neuroblastoma cell lines in vitro and in vivo. Acta Oncol 1999;38:1093–7.
26. Koopman G, Reutelingsperger CP, Kuijten GA, Keehnen RM, Pals ST, van Oers MH. Annexin V for flow cytometric detection of phosphatidylserine expression on B cells undergoing apoptosis. Blood 1994;84:1415–20.
27. Asahara T, Masuda H, Takahashi T, et al. Bone marrow origin of endothelial progenitor cells responsible for postnatal vasculogenesis in physiological and pathological neovascularization. Circ Res 1999;85:221–8.

INTERNATIONAL JOURNAL OF ONCOLOGY 24: 549-558, 2004

Gene therapy eradicating distant disseminated micro-metastases by optimal cytokine expression in the primary lesion only: Novel concepts for successful cytokine gene therapy

SATOSHI NAGANO[1,4,5], KENTARO YUGE[5], MARI FUKUNAGA[2], YASUHIRO TERAZAKI[2], HISAYOSHI FUJIWARA[6], SETSURO KOMIYA[4] and KEN-ICHIRO KOSAI[1,3,5]

[1]Division of Gene Therapy and Regenerative Medicine, Cognitive and Molecular Research Institute of Brain Diseases, Kurume University; Departments of [2]Surgery and [3]Pediatrics, Kurume University School of Medicine, 67 Asahimachi, Kurume 830-0011; [4]Department of Orthopaedic Surgery, Faculty of Medicine, Kagoshima University, 8-35-1 Sakuragaoka, Kagoshima 890-8520; [5]Department of Gene Therapy and Regenerative Medicine, Gifu University School of Medicine; [6]Cardiology, Respiratory and Nephrology, Regeneration and Advanced Medical Science, Graduate School of Medicine, Gifu University, 40 Tsukasamachi, Gifu 500-8705, Japan

Received October 1, 2003; Accepted November 18, 2003

Abstract. The most serious problem in current gene therapy is that clinical applications have often led to unsatisfactory results. Here we show novel concepts and crucial factors that have been missing for successful cytokine gene therapy. A clinically-relevant mouse model of primary and micro-metastatic osteosarcoma was generated by subcutaneously and intravenously injecting murine osteosarcoma LM8 cells, in which adenoviral gene transduction efficiencies were extremely low; current therapies remain less effective for such disseminated micro-metastases. A single injection of adenoviral vector encoding interleukin-2 gene (Ad.IL-2) was given only into the established primary tumor. Notably, antitumoral immunity was successfully elicited by IL-2 secretion from connective tissues adjacent to the primary tumor, and this immunity not only suppressed primary tumor growth but also eradicated disseminated micro-metastases in distant organs. Most importantly, not only minimal side effects but also maximal therapeutic effects were exerted only in the case of injecting the optimal (i.e., not the highest) dose of Ad.IL-2, because spleen injuries caused by excessive levels of circulating IL-2 might diminish the therapeutic effect. Although the narrow range of the optimal therapeutic expression level of IL-2 may be crucial, it was feasibly determined by serum IL-2 levels. Thus, a crucial factor for successful cytokine gene therapy is not the high gene transduction efficiency in the tumor, which has been generally recommended, but the use of the optimal therapeutic expression level. In conclusion, just a single injection of Ad.IL-2 into a primary tumor lesion, which is feasible, not invasive and cost effective, is potently therapeutic for distant disseminated micro-metastases, as long as the optimal therapeutic level is monitored. These novel concepts, which contradict those of previous studies, warn researches about the possible problems with the ongoing clinical cytokine gene therapy.

Correspondence to: Dr Ken-Ichiro Kosai, Division of Gene Therapy and Regenerative Medicine, Cognitive and Molecular Research Institute of Brain Diseases, Kurume University, 67 Asahi-machi, Kurume 830-0011, Japan
E-mail: kosai@med.kurume-u.ac.jp

Key words: adenovirus, cytokine, gene therapy, micro-metastases, osteosarcoma

Introduction

Cytokine gene therapy, which elicits a systemic antitumoral immune reaction, is a potential candidate that may evade the present technical obstacle of the limited gene transduction in tumors in clinical situations and that may treat non-transduced and disseminated cancer cells. We have shown the therapeutic potential of cytokine gene therapy with interleukin-2 (IL-2), granulocyte macrophage-colony stimulating factor and interleukin-12 used alone or in combination with suicide gene therapy for a variety of cancers using their clinically-relevant animal models (1-5). IL-2, which is one of the most widely studied cytokines, stimulates cytotoxic and helper T lymphocytes (6,7), natural killer cells (8-10) and lymphokine-activated killer cells, leading to activation of non-specific and specific responses to non-immunogenic tumors (11,12). Our previous studies using animal models that possess clinical characteristics demonstrated that IL-2 gene therapy was therapeutic for peritoneal dissemination of hepatocellular carcinoma (2); however, neither therapeutic effects nor an antitumoral immune reaction were elicited by IL-2 gene therapy used alone (that is, not in combination with suicide gene therapy) for some solid tumors (1,4,5). In contrast, many previous studies by other investigators simply showed tumor regression as the sole therapeutic effect in

simple animal models that do not reflect clinical situations, and some clinical trials may have been potentially performed based on such insufficient preclinical analyses. Generally, the most serious problem in current cancer gene therapy is that clinical applications have led to unsatisfactory results, although promising data were shown in experiments (13-18). We have recently found some crucial factors for successful suicide gene therapy (19,20). Likewise, we hypothesize that some crucial factors for successful clinical application of cytokine gene therapy have been missing, and that the therapeutic potentials of cytokine gene therapy have not been maximally utilized for suitable disorders based on this therapy's advantages and characteristics.

Osteosarcoma is one of the most frequent bone cancers in children (21,22), and despite aggressive conventional treatments, more than 30% of patients develop metastases, most frequently in the lung, within the first year after an initial diagnosis (23). Only 14-30% of patients survive 5 years once they have had lung metastasis, while the survival rate is 60-80% in the case of a tumor being localized in the limb without metastasis (23-26). This poor prognosis indicates an urgent need for the development of innovative and novel therapies for lung metastasis of osteosarcoma.

In this study, we explored whether a single injection of the optimal dose of adenoviral vector (Ad) encoding IL-2 gene (Ad.IL-2) only into the primary tumor lesion was an effective treatment not only for the primary tumor but also for disseminated micro-metastases of osteosarcoma in distant organs, in clinical-relevant animal models. We chose this treatment not only because Ad-mediated IL-2 gene therapy for the treatment of osteosarcoma has not yet been studied, but also, more importantly, because this is a good model to assess our three hypotheses regarding cytokine gene therapy. IL-2 was chosen as a therapeutic gene in the present study in terms of being representative in cytokine gene therapy. Our first hypothesis was that the main target of disseminated micro-metastases in distant organs may be curable by treatment of only the accessible primary tumor. Our second hypothesis was that high gene transduction efficiency in tumors, the requirement of which has been believed to limit the clinical utility of cancer gene therapy approaches in general, may not be necessary for cytokine gene therapy. Our third hypothesis was that the optimal expression level of a cytokine would be one that could draw out the maximal therapeutic effect rather than produce the minimal adverse side effects, and that optimum level might not be the highest one. Along with preclinical findings for the treatment of lung metastasis of osteosarcoma, the novel concepts shown in the present study is crucial for ongoing and future cytokine gene therapy in general.

Materials and methods

Cell lines. LM8, a murine osteosarcoma cell line with high metastatic potential to the lung, which was generated from the Dunn osteosarcoma cell line (27), was given by Dr H. Yoshikawa (Osaka University) and Dr A. Uchida (Mie University). Human osteosarcoma cell lines, NOS-2, U2OS and SaOS, were obtained from the RIKEN Cell Bank (Tsukuba, Japan), American Type Culture Collection (Rockville, MD) and the Cell Resource Center for Biomedical Research Institute of Development, Aging and Cancer, Tohoku University (Sendai, Japan), respectively. All these cell lines were maintained in α-minimum essential medium (Sigma-Aldrich, Tokyo, Japan) supplemented with 100 units/ml penicillin, 100 μg/ml streptomycin and 10% fetal bovine serum (Medical & Biological Laboratories Co., Ltd., Nagoya, Japan).

Recombinant adenoviral vectors (Ads). Ad.IL-2, replication-deficient Ad encoding the murine IL-2 gene driven by a modified chicken ß-actin promoter with cytomegalovirus enhancer (CAG promoter), was given by Dr H. Hamada (Sapporo Medical College) through the RIKEN Gene Bank (Tsukuba, Japan). Ad.LacZ and Ad.dE1.3, which contain the LacZ gene and no gene in place of the murine IL-2 gene, respectively, were generated as previously described (1). All Ads were amplified in 293 cells, purified on CsCl gradients twice and desalted by desalting column (Econo-Pac® 10DG, Bio-Rad Laboratories, Hercules, CA). The titer of Ad (plaque-forming unit (pfu)/ml) was measured by a plaque assay on 293 cells.

Adenoviral gene transduction efficiency in vitro. To determine adenoviral gene transduction efficiency in LM8, NOS-2, U2OS and SaOS cells *in vitro*, $3x10^5$ of these cells were infected with Ad.LacZ at various multiplicity of infection (MOI) for 1 h and media were sequentially replaced with fresh media. The cells were incubated for 48 h at 37˚C and sequentially fixed with 0.5% glutaraldehyde and stained with a solution containing 0.5 mg/ml 5-bromo-4-chloro-3-indolyl-ß-D-galactopyranoside (X-Gal, Wako Pure Chemical Industries Ltd., Tokyo, Japan), 13 mM $MgCl_2$, 15 mM NaCl, 44 mM HEPES (pH 7.4), 300 mM potassium ferricyanide and 300 mM potassium ferrocyanide. To evaluate adenoviral gene transduction efficiency, X-Gal-positive cells and total cells were counted in 20 microscopic fields under magnification x40, and the percentage of Ad-mediated gene transduction was calculated.

Animal model and experimental schedule. Our experimental schedule for working with animals is shown in Fig. 2. LM8 cells ($1x10^7$ cells) were injected subcutaneously into the back of 5-week-old male C3H/He mice. Subsequently, LM8 cells ($2x10^5$ cells) were injected via the tail vein at 6 days after tumor inoculation when the subcutaneous tumor became 5-6 mm in diameter, leading to 100% incidence of lung metastasis. At day 7 (1 day after intravenous injection of LM8 cells), all mice were randomly divided into 5 groups (5 mice in each group), and a single injection of Ad was given only into the subcutaneous primary tumor in 50 μl of 10 mM Tris-HCl (pH 7.4)/1 mM $MgCl_2$/10% (vol/vol) glycerol/Polybrene (20 μg/ml). Because all mice died several days after an injection of $3x10^8$ pfu of Ad.IL-2 into the primary tumor in a preliminary experiment, groups received the following respective injections in the present experiment: i) Ad.IL-2 ($1x10^8$ pfu), ii) Ad.IL-2 ($3x10^7$ pfu) + Ad/dE1.3 ($7x10^7$ pfu), iii) Ad.IL-2 ($1x10^7$ pfu) + Ad.dE1.3 ($9x10^7$ pfu), iv) Ad.dE1.3 ($1x10^8$ pfu) and v) vehicle. To ensure that the biological effect on tumor growth was due to the action of